DISSERTATION FOR THE DEGREE OF DOCTOR OF PHILOSOPHY (PHD)

THE IMPACT OF HEMOGLOBIN OXIDATION IN NLRP3 INFLAMMASOME ACTIVATION UPON INTRAVASCULAR HEMOLYSIS

by

BOGONKO BENARD NYAKUNDI

Supervisor: **Viktória Jeney PhD**

UNIVERSITY OF DEBRECEN

DOCTORAL SCHOOL OF MOLECULAR CELL AND IMMUNE BIOLOGY

DEBRECEN

2020

Table of Contents

INTRODUCTION

Red blood cells (RBCs) are the most abundant cell type in the human body with a lifespan of around 120 days. Hemoglobin (Hb) is the major component of RBCs, accounting for about 96% of the dry weight of the cells. Hb plays a key role in RBCs function as it binds oxygen molecules in the lungs and delivers it to the organs. Hb is build up by four subunits and each subunit is tightly associated with an iron-protoporphyrin IX (heme) prosthetic group. Because of high oxygen and iron content, RBCs are continuously exposed to a high level of oxidative stress that is counteracted by a highly efficient antioxidant network that protects Hb and the RBCs from extensive oxidation.

Aged RBCs are eliminated from the circulation efficiently and in an immunologically silent way by the reticuloendothelial system. On the other hand, growing evidence shows that extensive hemolysis that is a large scale uncontrolled destruction of RBCs within the blood vessels or in the extra-vasculature contributes largely to the pathologies of hemolysis-associated diseases, such as sickle cell disease or malaria. Studies showed that extracellular labile heme plays a key role in hemolysis-associated pathologies, through the activation of certain pattern recognition receptors (PRRs). In line with this notion, it has been shown that labile heme induces Toll-like receptor 4 (TLR4) and Nucleotide-binding domain, Leucine-rich Repeat containing protein 3 (NLRP3). Based on this phenomenon heme is considered as a damage-associated molecular pattern (DAMP).

Naïve Hb binds heme tightly, whereas oxidized Hb allows the release of heme due to structural distortions, therefore Hb oxidation precedes labile heme accumulation. Outside of the protective environment of RBCs Hb is susceptible to oxidation, leading to the formation of various Hb forms with different redox status of the heme iron (ferrous Fe^{2+}, ferric Fe^{3+} or ferryl Fe^{4+}), defining different Hb forms such as Hb (Fe^{2+}), metHb (Fe^{3+}) and ferrylHb (Fe^{4+}). Moreover, ferryl iron is a strong and unstable oxidant which decomposes through an intramolecular electron transfer while oxidizing specific adjacent amino acid residues of the globin chain. This leads to the formation of globin-based free radicals, which stabilize by sharing of their unpaired electrons forming covalent bonds between the Hb subunits.

We are lacking detailed information about (i) the production of these oxidized Hb forms, in particular ferrylHb, in the course of intravascular hemolysis (ii) and their potential role in the hemolysis-associated pro-inflammatory response. Therefore, in this study we investigated

the involvement of oxidized Hb forms in NLRP3 inflammasome activation and determined the potential contribution of these oxidized Hb forms in hemolysis-induced lethality. Additionally, using an *in vitro* approach we showed that after its formation, ferrylHb decomposes quickly and form covalently cross-linked Hb multimers.

LITERATURE REVIEW

1. Red Blood Cells (RBCs)

RBCs are distinguished by their biconcave disk shape and the capacity to endure the distortion while they circulate in the microvasculature. These cells are indispensable for the survival of humans as they facilitate the transport of oxygen from the lungs to the body tissues and take out carbon dioxide from tissues to the lungs. They are the most abundant cell type of the hematopoietic stem cell lineage with a lifetime of 110-120 days.

1.1. Erythropoiesis

RBCs originate in the bone marrow from the lineage-committed progenitor at the onset of erythropoiesis [3]. Hematopoietic stem cells give rise to burst-forming unit erythroid (BFU-E) progenitors which differentiate to colony-forming unit erythroid cells (CFU-E). CFU-E further generates proerythroblast, erythroblast, normoblast, and reticulocytes which move into the bloodstream to mature into erythrocytes **(Fig. 1)** [4].

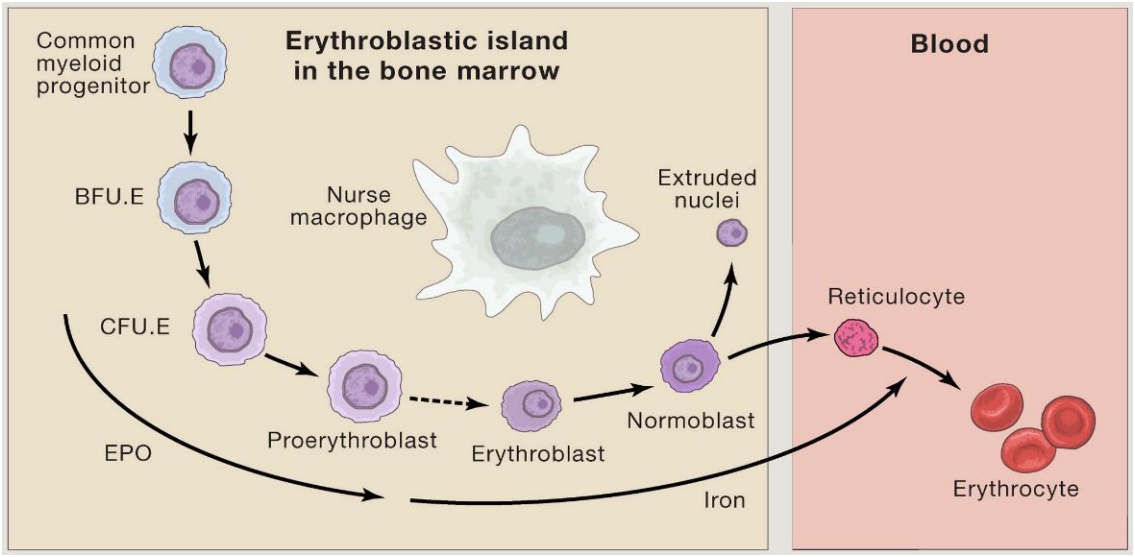

Figure 1. **Differentiation and maturing of RBCs**. In the bone marrow hematopoietic stem cells produce burst-forming unit erythroid cells (BFU-E) that advance to colony-forming unit erythroid cells (CFU-E). CFU-E progenitor cells generate erythroblastic islands around the central or 'nurse macrophage' within erythroid niche. Erythroblast then enucleate and move to the blood vessels as reticulocytes which eventually mature into erythrocytes. Modified from [2].

1.2. Hemoglobin is a major protein in the RBCs

The role of carrying O_2 and CO_2 of the RBCs in humans is facilitated by enclosed hemoglobin (Hb) molecules which occupy 96% dry weight of erythrocyte. Fetal hemoglobin (HbF) is the main oxygen carrier in the human fetus during the last 7 months of development in the uterus and remains the dominating Hb in the newborn until the age of approximately 6 months. In contrast to the adult form (HbA), which has a quaternary $\alpha_2\beta_2$ structure, HbF is composed of two alpha and two gamma chains [5]. Even though the overall structure shows strong similarities with that of HbA, the two Hbs exhibit some important differences in their biophysical properties [6]. The subunits in HbA are globular with a molecular weight of 16 kilodaltons (kDa), and each subunit contains a tightly bound non-protein part of iron-porphyrin IX known as heme [7]. Heme is a nearly plane circular tetra-pyrrole molecule, with a ferrous (Fe^{2+}) ion in the center that is coordinated with four nitrogen atoms of the pyrrols, and the N atom of the imidazole ring of F8 histidine residue of the globin chain. Because ferrous iron can coordinate six donor atoms, heme iron in the Hb has a vacant coordination site, allowing the reversible binding of one oxygen molecule [5, 7]. Oxidation states of heme iron are critically important in oxygen binding. In line with this notion, it is well established that metHb which contains ferric ion (Fe^{3+}) is unable to bind oxygen. Under homeostasis, metHb accounts for 1-2% of the total Hb content of RBCs which is produced by autoxidation of oxyHb yielding ferric iron and superoxide anion [8].

1.3. Antioxidant system of RBCs

Reactive oxygen species (ROS) production within the RBCs is a common phenomenon resulting from Hb autoxidation. Given the fact that the concentration of Hb in the RBCs can be as high as 5 mmol/L, a mere plodding rate of autoxidation could result in a pronounced ROS production. Consequently, erythrocytes are equipped with a highly efficient enzymatic and non-enzymatic antioxidant defense system to tackle the unfettered production of ROS [9]. RBCs contain Cu/Zn superoxide dismutase (SOD1) to convert superoxide anion to hydrogen peroxide (H_2O_2). The decomposition of H_2O_2 to H_2O is catalyzed by different enzymes including, catalase, glutathione peroxidase (Gpx-1) as well as peroxiredoxins (Prdx1 and Prdx2) [10]. Additionally, RBCs contain glutathione as the most important non-enzymatic ROS scavenger in RBCs [10].

The importance of this antioxidant defense system in the lifespan of RBCs was highlighted by recent studies where mice deficient of one of these particular enzymes such as SOD1, Prdx1, and Prdx2 manifested ROS accumulation together with hemolytic anemia [11-13]. On the

other hand, neither Gpx-1 nor catalase deficient mice showed evidence of elevated ROS production and subsequent perturbation of RBCs life span [9, 14].

Besides ROS, autoxidation of Hb yields metHb which needs to be converted back to Hb to keep the oxygen-binding capacity of RBCs high. This conversion is catalyzed by metHb reductase which is an integral part of the antioxidant defense system in RBCs [15]. Finally, there is an emergent observation that Hb has inherent antioxidant properties, attributed to the β93 cysteine, an evolutionarily conserved residue among the vertebrates. This cysteine residue has been implicated in lowering the rate of autoxidation of the β chain and in preventing heme degradation by scavenging of superoxide [16, 17].

1.4. Aged RBC clearance and decomposition

As mentioned earlier, human RBCs have a life span of about 120 days, and around 40 days in mice. Every day, a staggering number of erythrocytes, about 200 billion, are produced and cleared to maintain the physiological balance. The clearance of senescent RBCs is accomplished by macrophages commonly found in the spleen and the bone marrow, in a process called erythrophagocytosis [18].

The phenotype of senescent RBC is characterized by decreased metabolic activity and membrane remodeling, resulting in smaller and denser RBCs [19]. Specific cell surface markers identify aged RBCs for phagocytosis which appear suddenly at the terminal stage of the aging process, most likely just before the phagocytosis [20]. Because RBCs cannot synthesize new proteins, we can assume that the removal signals emerges due to the modifications in pre-existing molecules [18]. Removal signals include flipped phosphatidylserine and phosphatidylethanolamine, diminished expression of membrane sialic acid, and decreased expression of CD47 with the association of reduced membrane fluidity [21, 22]. To date, several mechanisms have been proposed for the clearance of senescent RBC by macrophages including Band-3-mediated and phosphatidylserine receptor-mediated processes.

Band-3, an abundant RBC transmembrane protein, has been implicated in the clearance process of senescent RBCs. Band-3 is a target of naturally occurring IgG antibodies which upon binding to Fc receptors on phagocytotic cells can initiate erythrophagocytosis [23-25]. Naturally occurring anti-band-3 antibodies are not efficient opsonins, but they have a unique affinity for C3, therefore it is assumed that this pathway works more efficiently when the classical pathway of the complement system is activated [26]. Phosphatidylserine, a phospholipid component of the cell membrane is normally found on the inner leaflet of the membrane. Upon apoptosis, phosphatidylserine flipping occurs and exposed at the cell surface

and serves as an “eat me” signal for phagocyte recognition resulting in a non-inflammatory clearance of the dying cell [27]. Similarly to that of apoptotic cells, aged RBCs exhibit the increased presence of phosphatidylserine on the cell surface which correlates to the RBC clearance from the circulation [28]. Various receptors have been identified on phagocytes that recognize phosphatidylserine on the cell surface including Tim1, Tim4, and Stabilin-2 [29, 30]. These receptors play a critical role in the phagocytosis of phosphatidylserine positive cells including aged RBCs.

Eventually, the phagosomes and senescent RBCs merge with lysosomal vesicles to form erythrophagolysosomes where senescent RBCs are broken down. The globin part is cleaved and heme is exported to the cytosol by the heme transporter protein known as heme responsive gene 1 protein [31].

1.5. The importance of RBC iron recycling in systemic iron metabolism

The total iron body content is about 3-5 g in the average human adult. Almost two-thirds of the total iron atoms are contained in Hb and myoglobin in the form of heme. The lost iron through the shedding of the skin, mucosal cells, and sometimes loss of blood is replenished through daily dietary uptake of 1-2 mg of iron augmenting recycled iron from senescent RBCs to maintain the daily body requirement of iron [32].

Iron metabolism is fundamental in a lifespan of RBCs and in most cases, the recycled iron from senescent RBCs is sufficient for the synthesis of Hb [4]. Following erythrophagocytosis, iron is liberated from heme by heme oxygenase-1 (HO-1) in the cytosol [33], and, depending on the actual needs for iron, is either stored or transported out of the macrophage. Ferritin is the major storage molecule in which iron is stored in the cytosol in a non-redox active form [34]. Ferritin is composed of 24 subunits of two kinds; heavy (FtH) and light (FtL) chains to form a globular protein with the capacity to accommodate 4500 iron atoms [34]. Alternatively, iron is exported out from macrophages by ferroportin to meet the physiological need, particularly the production of RBCs [35]. It has been established that a high level of iron triggers the release of hepcidin hormone which in turn leads to the internalization and degradation of ferroportin, hence preventing the release of iron from the cells [36]. On the other hand, a decreased level of iron triggers the withdrawal of hepcidin from the circulation to allow the release of iron [36].

Transportation of iron in the plasma is accomplished by transferrin that has two binding sites for ferric iron. Importantly, transferrin-bound iron is catalytically inactive therefore transferrin prevents the deleterious effects of iron. Di-ferric transferrin binds to transferrin

receptor 1 (TFR1) that is highly expressed on the surface of erythroid progenitor cells leading to endocytosis of the receptor-ligand complex and subsequent release of iron from transferrin, a process that is boosted by the acidic environment in the late endosome [4, 37].

Following the dissociation of iron from transferrin, iron is transported out from the endosome through divalent metal transporter 1 to the cytosol [4]. Most of the iron in the erythroid progenitors are used for heme biosynthesis, therefore, iron enters the mitochondria through mitoferrin 2 and then inserted into the protoporphyrin IX ring through the action of ferrochelatase [38, 39]. Heme is transported out of the mitochondria to the cytosol through Feline leukemia Virus subgroup receptor 1b (FLVCR1b) transporters for the completion of Hb synthesis, while excess heme is exported out from the cell by FLVCR1a [40].

2. Hemolysis

Hemolytic anemia occurs when the membrane of the RBCs prematurely raptures and releases its cytoplasmic content to the surrounding. Destruction of RBCs may take place in the blood vessels termed as intravascular hemolysis (IVH) which is clinically manifested by hemoglobinemia and may be accompanied by hyperbilirubinemia.

2.1. Causes of hemolysis

Sickle cell anemia, a genetic condition where normal RBCs are sickled due to a point mutation resulting from a replacement of glutamic acid by valine amino acid in the β chain causes intravascular hemolysis [41]. Besides, other genetic hemoglobinopathies that lead to premature destruction of RBCs, affect the membrane of the RBCs, for example, genetic spherocytosis and genetic elliptocytosis [42].

Furthermore, enzymopathies in defective metabolic RBCs play a role in hemolytic anemia. RBCs with defective enzymes never show morphological changes but there is always a fluctuation of ATP production depending on the relative importance of the affected enzyme. The depletion of ATP triggers a cascade of events leading to hemolysis. ATP-deficient RBCs lose water and potassium making them rigid and dehydrated hence increased intracellular acidity, hypoxia, and stasis resulting in the inhibition of the glycolytic pathway. Ultimately, the cells with defective enzymes are entrapped and destroyed in the vasculature of the spleen and liver. Some of the enzyme deficiencies involved in metabolic-related hemolysis include glucose 6-phosphate dehydrogenase, pyruvate kinase, and aldolase [43, 44].

On the other hand, other non-genetic hemolytic factors can induce hemolysis including physical trauma, complement activation, pathogen-induced lysis as in malaria, immune-

mediated hemolysis in agglutinins syndrome, drug-activated hemolysis, and ABO cross-reaction resulting from blood transfusion [45-47].

Extravascular hemolysis essentially occurs when RBCs are unable to change their shape as they flow through the narrow capillaries. Sickle cell anemia or cellular hydration condition such as hereditary spherocytosis and elliptocytosis reduce the deformability of RBC facilitating their destruction by the spleen macrophages [48]. The spleen plays a role in safeguarding the quality of the RBCs by letting the cells pass through a constricted inter-endothelia slits of red pulp and consequently entraps all defective cells [49].

2.2. Haptoglobin- hemopexin heme oxygenase-1 ferritin defense system

Outside of the protective environment of RBCs Hb is prone to oxidation and subsequent heme release [10]. Therefore, extracellular Hb and oxidized Hb forms, together with heme require efficient clearance mechanisms to limit their harmful effects **(Fig. 2)**. In the circulation acellular Hb scavenges the crucial vasodilator nitric oxide leading to reduced smooth muscle cell relaxation [50]. Cell-free Hb forms and free heme can trigger prothrombotic, pro-inflammatory, and pro-oxidant responses by targeting different cell types of the vasculature such as blood leukocytes and endothelial cells [51-54].

Haptoglobin (Hp) is the first line of defense that evolved to prevent the accumulation and pro-oxidant effects of acellular Hb. Hp is a tetramer with 2α chains and 2β chains (2α2β), which are interconnected by disulfide bonds [55, 56]. However, electron microscopic analysis of purified Hp from patients revealed Hp polymorphism in humans [57]. The structural heterogeneity is determined by critical disulfide linkages found in alpha chain Hp which is necessary for covalent crosslinking of Hp monomers. Hp 1-1 is monovalent, while Hp 2-1 is bivalent which means it can form linear polymers and Hp 2-2 is capable of forming cyclic polymers [57]. Hp-Hb association is one of the strongest non-covalent bonds enabling the removal of Hb from plasma in a ratio of 1:1 though it has been shown that Hp 2-2 has a lower affinity to Hb as compared to Hp 1-1 [57, 58]. Hp-Hb complexes are bound to Hp receptor CD163 on macrophages subsequently initiating receptor-mediated endocytosis. Additionally, Hb can interact directly with CD163 receptors enabling a salvage pathway for Hb removal in the absence of Hp, though this pathway has low efficiency [55, 59].

The Hb-binding capacity of Hp can be overwhelmed upon massive hemolysis under pathologic conditions [60], leading to the accumulation of extracellular Hb which oxidizes and releases heme group [61]. The free heme is bound by a host of plasma proteins including hemopexin (Hx), albumin, α_1-microglobulin, and lipoproteins that form the second defense line against hemolysis [62-65]. Hx is a major acute-phase protein with the highest affinity ($K_d < 10^{-12}$ M in humans) for heme. The binding of Hx to heme inhibits the pro-oxidant activity of heme. Moreover, the heme-Hx complex is recognized by CD91 receptors expressed mainly on macrophages and hepatocytes, which mediate heme clearance via receptor-mediated endocytosis [66-68]. Deficiency of the two critical plasma proteins Hp and Hx involved in Hb and heme clearance respectively increased the susceptibility to hemolytic stress in a mice model, demonstrating the concerted role of these proteins in the clearance of extracellular Hb [69, 70].

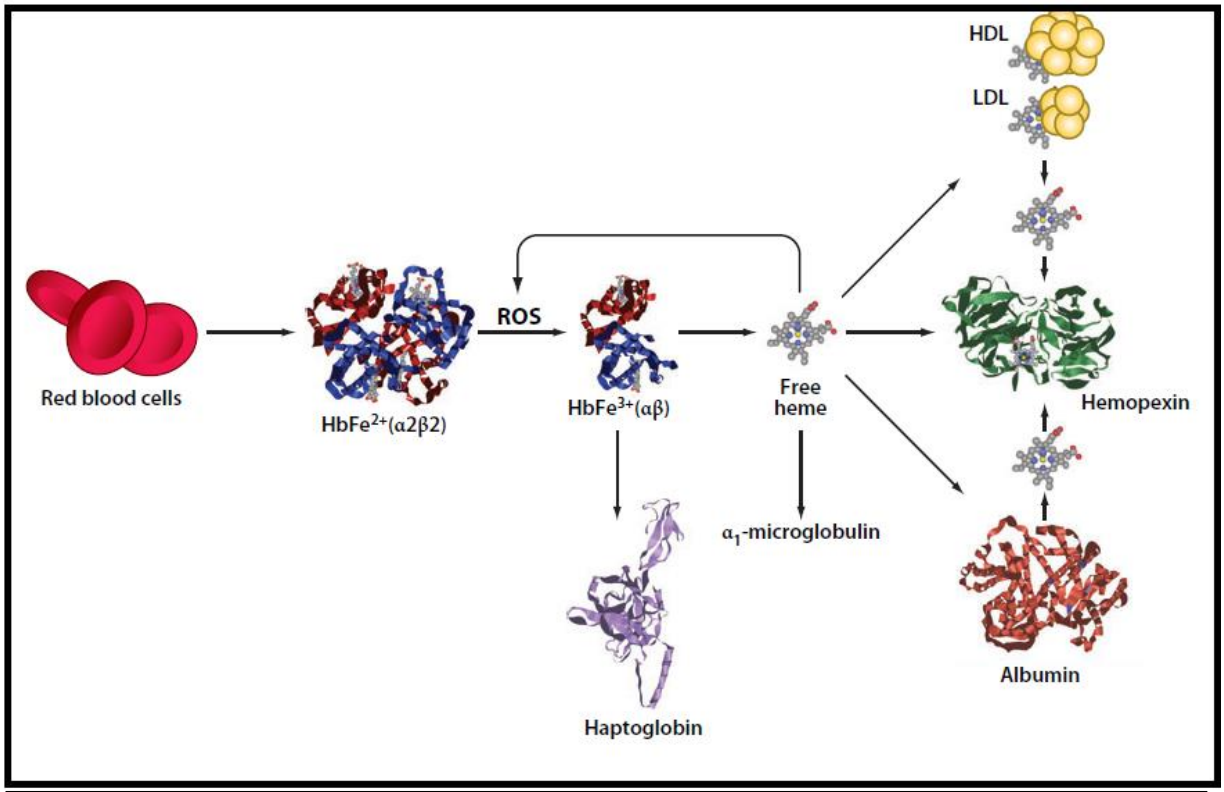

Figure 2. Controlling of extracellular Hb and heme. In physiological conditions acellular Hb released from RBCs is cleared by haptoglobin (Hp). Upon severe hemolysis Hp is depleted from the circulation leading to Hb accumulation, oxidation and subsequent release of heme. Heme is scavenged by plasma proteins such as hemopexin (Hx), α_1 microglobulin, albumin and lipoproteins (LDL and HDL). Hx possesses the highest affinity ($K_d \sim 10^{-12}$ M) towards heme and it acts as a major heme scavenging molecule. Adapted from [2].

Following its uptake through CD91, heme is degraded in the cytosol by heme oxygenases (HOs). HO enzymes break down heme into equimolar amounts of iron, carbon monoxide (CO), and biliverdin **(Fig. 3)** [71]. HO-1, the inducible isoform of the HO enzymes is induced by a variety of stimuli such as heme, oxidative stress, certain hormones, and metals. Because its expression is avidly regulated by heme, this enzyme plays a major role in heme detoxification [72]. Beyond degrading the potentially harmful heme molecule, the HO-1-induced heme breakdown has other cytoprotective functions that rely on the antioxidant and anti-inflammatory activities of the products of heme degradation [73-75]. After its production, biliverdin (BV) is converted into bilirubin (BR) by biliverdin reductase (BVR). Bilirubin is an antioxidant and exhibits cytoprotective effects [75]. The other product of heme degradation is CO that is an important gasotransmitter with strong antioxidant and anti-inflammatory properties [76]. Besides HO-1, heme induces the expression of ferritin that stores the liberated iron in a redox inactive form, thus preventing its involvement as a catalyst in Fenton reaction [77].

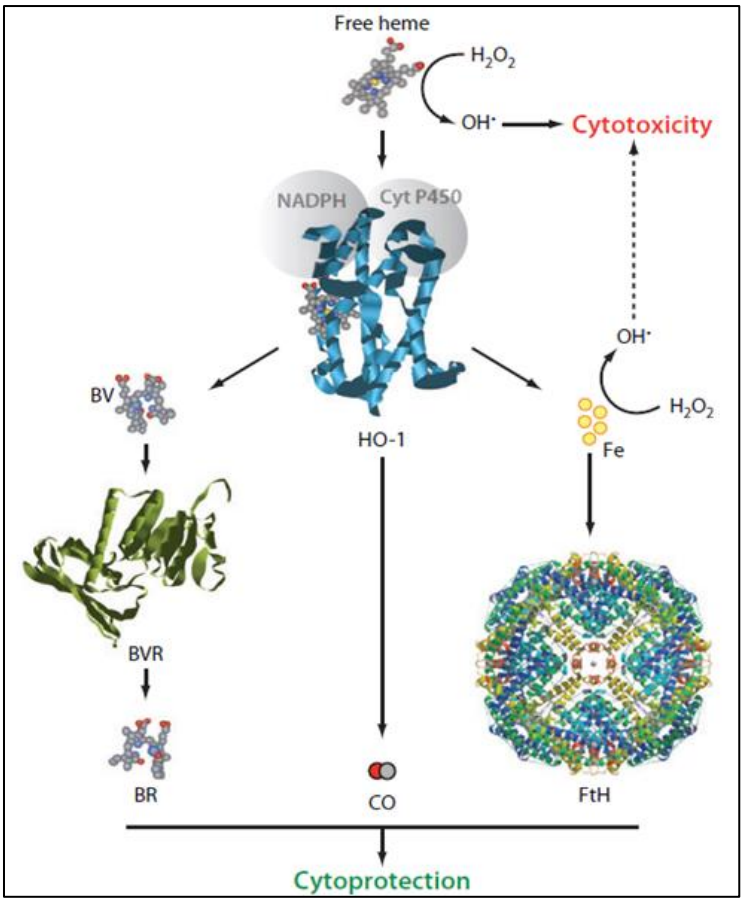

Figure 3. Breakdown of heme by HO-1. HO-1 cleaves heme into biliverdin (BV) and carbon monoxide (CO) with the concomitant release of iron. The iron (yellow dot) is stored by ferritin. BV is reduced to bilirubin (BR) by biliverdin reductase (BVR). BR, CO and FtH possess diverse antioxidant anti-inflammatory and cytoprotective effects. Adapted from [2].

2.3. Hemoglobin oxidation

Under physiological conditions, iron exists in two stabile oxidation states, Fe^{2+} (ferrous) and Fe^{3+} (ferric). In the heme molecule, iron exists in the ferrous oxidation state, however, oxygen-binding can trigger autoxidation of heme iron into a ferric ion with the concomitant production of superoxide anion (equation 1). This reaction is under control in intact RBCs via the action of the antioxidant system in RBCs (discussed previously). Following massive intravascular hemolysis, when the Hb scavenging capacity of plasma is overwhelmed Hb quickly oxidizes to ferric and ferryl (Fe^{4+}) states producing metHb and ferrylHb, respectively [10]. FerrylHb is formed in two-electron oxidation of Hb that can be triggered by H_2O_2 or lipid hydroperoxides (equation 2). On the other hand, the reaction between H_2O_2 with metHb produces ferrylHb radical (equation 3) in which the unpaired electron can be associated with either the globin chain or the porphyrin ring [78, 79].

(1) $Hb(Fe^{2+})O_2 \rightarrow Hb(Fe^{3+}) + O_2^{\bullet-}$

(2) $Hb(Fe^{2+})O_2 + H_2O_2 \rightarrow Hb(Fe^{4+}= O^{2-}) + H_2O + O_2$

(3) $Hb(Fe^{3+}) + H_2O_2 \rightarrow Hb^{\bullet+}(Fe^{4+}= O^{2-}) + H_2O$

(4) $Hb(Fe^{4+}= O^{2-}) + 2H^{+} \rightarrow Hb^{\bullet+}(Fe^{3+}) + H_2O$

(5) $Hb^{\bullet+}(Fe^{3+}) + Hb^{\bullet+}(Fe^{3+}) \rightarrow (Fe^{3+})\ ^{+}Hb\text{-}Hb^{+}(Fe^{3+})$

Further metHb globin radicals can be formed through intramolecular electron transfer between the ferryl iron and adjacent amino acid residues of the globin subunit (equation 4). The termination reaction between these globin radicals results in covalent cross-linking of the globin chains (equation 5).

Amino acids in both alpha and beta-globin subunits have been identified as targets of ferryl-iron triggered oxidation and radical formation. In a study where Hb was reacted with H_2O_2 in the presence of spin trap 5,5-dimethyl-1-pyrroline N-oxide, adducts from both alpha and beta chains were trapped. Further studies identified the amino acids where radical formation occurred during H_2O_2-induced Hb oxidation, which include βCys93, αTyr24, αTyr42, and αHis20 residues of the globin chains [54, 80, 81].

Additionally, Hb oxidation can lead to the formation of hemichromes (**Fig. 4)**. Hemichromes are defined as oxidized low-spin metHb species whose formation usually precedes Hb denaturation [82]. Hemichromes have two types, reversible hemichromes that keep their ability to return to Hb, and irreversible hemichromes that cannot be converted back to Hb.

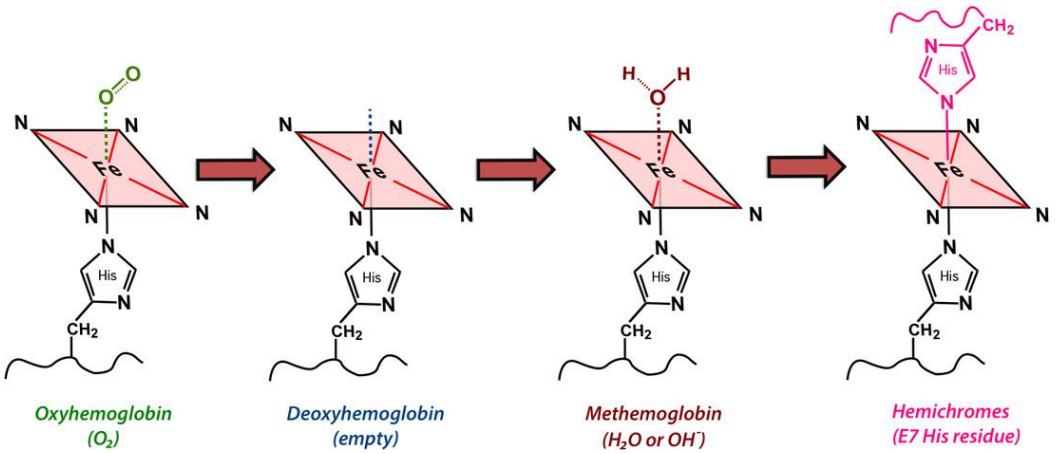

Figure 4. Structure of different Hb species. The structures of oxyHb, deoxyHb, metHb, and hemichromes. The iron (Fe) center has 6 potential coordination sites, four of which are occupied by porphyrin nitrogens (N). The fifth coordination site (below the plane of the ring) covalently bonds with a histidine (His) residue from the F8 position of its respective globin chain. The sixth coordinate (above the plane) is the oxygen binding site. Figure is adapted from http://mriquestions.com/types-of-hemoglobin.html.

2.4. Presence of oxidized Hb forms in vivo

The formation of the highly oxidized (ferryl) Hb forms and globin radicals under *in vivo* conditions was debated for a long time because these molecules are transiently formed due to their high reactivity. Svistunenko et al. provided the first evidence by detecting ferrylHb globin-centered radicals in normal human blood by electron paramagnetic resonance spectroscopy [79]. In another study, an oxidized Hb form which was characterized by the presence of a covalently modified heme prosthetic group was detected. It was also shown that the concentration of this oxidized Hb form is increased by exercise, a surrogate model of acute oxidative stress [83].

Oxidation of Hb has been shown in certain pathological conditions. For example, heme-protein cross-linked Hb was detected in cerebrospinal fluid following subarachnoid hemorrhage [84]. Moreover, recently it was found that the content of dityrosine is elevated and globin-globin cross-linked Hb multimers are present in complicated atherosclerotic lesions in humans [85].

3. The danger theory

Between the 1960s and 1990s, immunologists proposed an immune response theory of "self-non-self" which states that immune response is triggered against all foreign (nonself) substances while the organism's components do not provoke an immune response [86]. In 1994, Polly Matzinger postulated a rival theory called the "danger theory" suggesting that the immune response is triggered by "danger signals" or "alarm signals" released by an organism's cells. In line with this theory, the immune response is due to the releasing of "danger signals" within the organism but not "nonself" (genetically foreign entities) [87, 88]. Since the fundamental statement of the "danger theory" suggests that immune responses are due to tissue damage rather than "danger", the theory was later on more precisely designated as "damage theory" rather than "danger theory" [89]. Kono and Rock proposed four features as a basis of evaluating damage-associated molecular patterns (DAMPs): (1) DAMPs should be active as highly purified molecules; (2) biological activity of DAMPs should not be attributable to the contamination of pathogens; (3) the DAMP should be active at the concentrations that are present in pathophysiological settings; (4) discreet elimination or inactivation of the DAMPs should inhibit the biological activity of dead cells *in vitro* or *in vivo* [90]. The authors acknowledge that maybe not all the DAMPs meet all the above-mentioned criteria, but these criteria could serve as a blueprint for further research.

3.1. Categories of DAMPs

It is now established that various DAMPs that could be released by damaged or dying cells have the potential to trigger an immune response [91]. In the absence of foreign substances, stress signals were first identified as DAMPs upon their release by necrotic cells due to the ungoverned disruption of the plasma membrane. These stress signals activate antigen-presenting cells [92]. Upon tissue damage, extracellular proteins such as hyaluronan and proteoglycans are released from the extracellular matrix and serve as DAMPs [93]. On the other hand, intracellular proteins from various cell compartments can be released and behave as DAMPs upon cell damage/stress. These DAMPs include histone proteins and nuclear proteins such as high mobility group box-1 originating in the nucleus [94], ATP, and mtDNA from the mitochondria [95], and cytosolic molecules including heat shock proteins and uric acid [96, 97]. Additionally, endogenous and exogenous crystals of diverse architecture trigger the immune response in chronic inflammatory diseases. Examples for endogenous crystals include cholesterol crystals associated with atherosclerosis, monosodium urate crystals in gouts, calcium pyrophosphate dihydrate crystals in the case of pseudogout, and amyloid fibril

in Alzheimer disease [98-101]. Exogenous particles such as silica and asbestos play a role in silicosis and asbestosis respectively [102, 103].

Physiologically, the majority of cytosolic molecules are kept in reduced states to maintain their functionality. Some of the molecules that are released upon cell damage/stress are converted into DAMPs in the extracellular milieu due to conformational changes triggered by oxidative stress outside of the cytosol. Hb is a typical example of a protein that is kept in a reduced stable state until it is compartmentalized in RBCs but becomes a DAMP once outside of the protective environment of RBCs due to oxidation and conformational changes [91, 104].

3.2. DAMPs sensors

The immune system detects DAMPs by engaging a cluster of germline-encoded pattern recognition receptors (PRRs) which are expressed both in immune and non-immune cells. Based on their location, PRRs can be membrane-bound such as toll-like receptors (TLRs) or cytosolic, such as NOD-like receptors (NLRs) [105]. The recognition of DAMPs by PRRs initiates signaling events intended to clear the DAMPs and to promote the healing process.

By definition, TLRs are membrane-bound PRRs belonging to a family of type-1 transmembrane receptors which are characterized by leucine-rich repeat (LRR) domain and an intracellular Toll/IL-1 receptor (TIR) domain [106]. Up to date, 10 subtypes of TLRs have been identified in mammals with diverse ligand specificity. Upon ligand binding, TLRs dimerize, recruit adaptor molecules which in turn trigger a cascade of events that in most cases will eventually lead to the translocation of nuclear factor kappa B (NF-κB) to the nucleus and initiate the expression of target genes [107, 108].

The NLRs is a vast family of intracellular PRR comprising of at least 22 and 33 members in human and mice, respectively. There are three common structural domains in the NLRs that include; C-terminal LRR domain, a central nucleotide-binding oligomerization domain NOD or NACHT and N-terminal caspase recruitment (CARD) or pyrin (PYD) domain for mediating protein-protein interaction to enhance downstream signaling, and at the same time CARD or PYD domains are used to determine the subgroups of NLRs [109, 110]. Various subgroups of NLRs including NLRP3, form a cluster of proteins complexes upon the detection of DAMPs and/or PAMPs, prominently known as inflammasomes. These molecular platforms are comprised of a sensor molecule, an adaptor protein apoptosis-associated speck-like protein containing a caspase recruitment domain (ASC), and an effector caspase-1 enzyme. The activation of the sensor protein, connects with the PYD domain of ASC adaptor. Subsequently, ASC bind with pro-caspase-1 through the CARD domain. The assembly enhances cleavage of

pro-caspase-1 to active caspase-1 which in turn cleaves pro-IL-1β and pro-IL-18 to active pro-inflammatory cytokines [111, 112].

The NLRP3 inflammasome complex is one of the best characterized NLR, partly because of its well-defined activators. In general, the NLRP3 inflammasome is activated by two signals where the first signal leads to the activation of NF-κB pathway, and the transcription of pro-IL-1β whereas the second signal comprises of a wide range of PAMPs and stress-related signals or DAMPs that initiate the assembly of the inflammasome complex [113-115]. The three mechanisms through which NLRP3 have been proposed to be activated involve potassium efflux, ROS generation, and the release of cathepsin B [116].

4. RBC-derived DAMPs

In general, intravascular hemolysis is a silent event, without any inflammatory reaction. On the other hand, massive intravascular hemolysis, − when the clearing capacity of plasma is overwhelmed − associates with a sterile inflammatory response. Growing evidence suggests that lysing RBCs release several components that are recognized as DAMPs by inflammatory cells as shown in Table 1 below [117].

Table 1. RBC-derived DAMPs and proposed respective receptors

Red cell DAMPs	Role/function in RBC	Associated receptors
Heme	Released following oxidation of cell-free hemoglobin	TLR4 and NLRP3
Hsp70	Molecular chaperone	TLR2, TLR4, CD14
ATP	Energy source, released from RBC during cell damage, hypoxia, reduced oxygen tension and oxidative stress	NLRP3 and P2X7
mtDNA	Residual (from reticulocytes)	TLR9, NLRP3
Cyclophilin A	Chaperone found in the cytosolic fraction (residual from reticulocytes)	CD147
IL-33	Stored in the RBCs	ST2

Note CD147: Cluster of Differentiation 147 ST2: Suppression of Tumorigenicity 2. Source:[117]

4.1. Hemoglobin/Heme

Upon massive intravascular hemolysis, a large amount of Hb is released to the circulation exceeding the clearing capacity of Hp. Hb oxidation occurs followed by heme release. When

the heme scavenging potential of Hx is overwhelmed labile heme accumulates in the plasma. Many studies addressed the pro-oxidant and pro-inflammatory effects of labile heme, as the major hemolysis-associated DAMP. The pro-inflammatory actions of the upstream oxidized Hb forms are much less known.

4.2. Heme as a TLR4 ligand

Figueiredo et al. showed that heme induces tumor necrosis factor-alpha (TNF-α) secretion in macrophages. They found that this response is dependent on TLR4, as macrophages derived from TLR4 deficient mice did not respond to heme treatment [118]. They also showed that the coordinated iron and the protoporphyrin IX ring together triggers the immune response, as macrophages were not induced by either iron or protoporphyrin IX [118]. Furthermore, Fortes et al. showed that exposing macrophages to free heme triggers programmed macrophage necrosis through TLR4/Myd88-dependent release of TNF-α and a TLR4-independent generation of ROS in a synergistic manner [51]. The role of TLR4 in heme-mediated inflammation was further proved by Lin et al. in a mouse model of intracerebral hemorrhage-induced neuro-inflammation. They found less inflammation, reduced cerebral edema, and lower neurological deficit scores in TLR4 deficient mice as compared to wild type mice, suggesting that heme-mediated TLR4 activation plays a crucial role in intracerebral hemorrhage-associated neuroinflammation [119].

Besides macrophages, TLR4 has been shown to play an important role in heme-mediated endothelial cell activation. Endothelial cells form a physical barrier between blood and tissues, preventing the transmigration of inflammatory cells to the tissues. On the other hand, inflammatory stimuli activate endothelial cells leading to the upregulation of adhesion molecules that initiates leukocyte adhesion and extravasation of inflammatory cells to the inflamed tissue [120, 121]. It has been shown that heme also upregulates the expression of adhesion molecules in endothelial cells [122], and recent evidence suggests that heme-mediated endothelial activation happens in a TLR4-dependent manner. Belcher et al. showed that heme-mediated TLR4-dependent endothelial activation plays a pathogenic role in sickle cell disease [123].

4.3. Heme as an inducer of NLRP3 inflammasome

Besides being a TLR4 ligand, heme has been recently recognized as an inducer of NLRP3 inflammasome activation. Dutra et al. showed that heme induces the release of IL-1β from LPS-primed macrophages [1]. Heme-mediated IL-1β production is dependent on caspase-1 and NLRP3 as neither caspase-1 deficient, nor NLRP3 deficient mice respond to heme treatment

[1]. Similar to TLR4 activation, NLRP3 activation requires structural integrity of the heme molecule, as neither iron nor protoporphyrin IX induced IL-1β production in LPS-primed macrophages [1]. On the contrary, Li et al. showed that protoporphyrin IX induces maturation and secretion of IL-1β in LPS-primed macrophages similar to that of heme [124].

Dutra et al. proposed a mechanism of heme-induced NLRP3 inflammasome activation in macrophages where they suggested that the release of IL-1β requires two signals. The first signal is related to PAMPs such as LPS or TNF which activates the macrophages via TLR or TNF receptor 1 (TNFR1) respectively, to induce the translocation of NF-κB to the nucleus which in turn initiate the transcription of Pro-IL-1β, caspase-1, and NLRP3 genes.

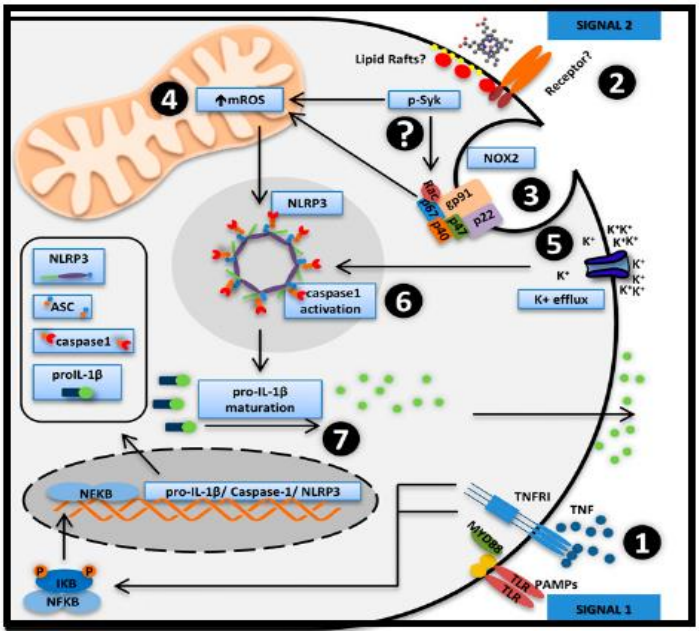

Figure 5. Mechanisms of heme-mediated NLRP3 inflammasome activation in macrophages (1) Macrophages are primed by PAMPs like LPS or TNF to activate NF-κB nuclear translocation and induce the expression of pro-IL-1β, caspase-1, and NLRP3. (2) Heme induces phosphorylation of spleen tyrosine kinase (Syk) either through the reorganization of lipid rafts or through a currently unknown receptor. Heme triggers mtROS production and NLRP3 inflammasome activation via Syk. (3) Heme activates NOX2 that is crucial in the production of mtROS and NLRP3 activation. (4 and 5) Generation of mtROS and K^+ efflux are essential in heme-induced inflammasome activation. (6) Heme activates NLRP3 inflammasome assembly through mtROS, NOX2, and K^+ efflux. (7) Caspase-1 cleaves inactive pro-IL-1β to active secreted IL-1β. Adapted from [1].

Heme act as a second signal either through cell membrane alterations [125], or through some undetermined receptors, and triggers the phosphorylation of spleen tyrosine kinase (Syk). Heme induces NADPH oxidase 2 that is essential in the production of mtROS but also heme triggers K^+ efflux. Jointly, the generation of mtROS and K^+ efflux initiate the assembling of

NLRP3 inflammasome. The inflammasome activates caspase-1 which eventually cleaves pro-IL-1β to a mature IL-1β **(Fig. 5)** [1].

4.4. Other RBC-derived DAMPs

Besides Hb-derived DAMPs, RBCs have other components capable of becoming DAMPs following severe hemolysis. For instance ATP, a universal energy currency is present in the RBCs at a concentration of about 1.6 mmol/L that is released upon hemolysis [126]. ATP binds to P2-purinergic receptors and triggers inflammatory responses in various immune and non-immune cells [127, 128]. For example, ATP activates P2X purinoceptor 7 (P2X7) consequently boosting the release of proinflammatory cytokines IL-1β and IL-18 in LPS-primed macrophages [129]. It was further shown that ATP triggers the release of microparticles (MPs), generation of ROS, and triggers apoptosis in erythroid progenitor cells [130-132].

IL-33 is a member of IL-1 superfamily broadly expressed within mucosal tissues and a putative alarmin released upon cellular trauma contributing to the pathogenesis of various inflammatory diseases by activation of innate immunity [133]. RBCs contain IL-33 that is released upon RBC lysis [134, 135]. IL-33 exerts its deleterious effects through ST2 receptors and influence different lymphoid and myeloid immune cells [136].

Microparticles are phospholipid membrane-bound vesicles of less than 1 μm in size released into the body fluids by different cells such as endothelial cells, RBCs, leukocytes, or platelets following cellular stress, activation of cells, and apoptosis [137]. Hb disorders like sickle cell disease and thalassemia major are commonly typified by shortened RBCs life span that correlates with the accelerated formation of RBC-derived microparticles [138]. RBC-derived microparticles exert diverse biological effects such as scavenging of NO from the vasculature, augmenting of systemic inflammation through thrombin-dependent activation of the complement system, and endothelial activation via heme transfer [139-141]. Myeloid lineage cells uptake RBC-derived microparticles leading to the subsequent release of pro-inflammatory cytokines [142].

AIMS

Labile heme is a well-established DAMP, a ligand for TLR4, and an inducer of NLRP3 inflammasome activation. Heme is considered to play a major role in hemolysis-associated inflammation and organ damage. On the other hand, a recent study highlighted that IVH-induced renal alterations are largely heme-independent because the administration of free heme could not trigger them, and heme scavenging could not prevent them either [143]. This postulated that maybe upstream hemolysis-derived products contribute to the detrimental effects of massive hemolysis. Our aim in this work was to provide a detailed analysis of extracellular heme forms following IVH and to investigate the contributions of these heme forms to hemolysis-associated inflammation, particularly NLRP3 inflammasome activation and subsequent production of IL-1β.

To accomplish this aim we wanted to answer the following questions:

1. What kinds of Hb species can be detected in the mice plasma following PHZ-induced IVH?
2. Does PHZ-induced IVH trigger IL-1β production *in vivo*?
3. Which Hb redox forms induce IL-1β production in macrophages *in vitro*?
4. Which Hb redox forms behave in a pro-inflammatory manner *in vivo*?
5. Is IVH-induced IL-1β production dependent on NLRP3 inflammasome activation?
6. If NLRP3 deficiency provides a survival advantage to mice is it associated with increased resistance or increased tolerance to IVH?
7. How and how fast ferrylHb is decomposed after its formation?

MATERIALS AND METHODS

Materials

Reagents were purchased from Sigma-Aldrich (St. Louis, MO, USA) unless otherwise specified.

Hb preparation

Hb at different redox states Hb, metHb, and ferrylHb was prepared from fresh blood drawn from healthy individuals. The isolation of Hb was performed by the use of ion-exchange chromatography on a DEAE Sepharose CL-6B column (Sigma-Aldrich). We generated metHb by incubating purified Hb with a 1.5-fold molar excess of $K_3Fe(CN)_6$ over heme for 30 min, at 25°C. FerrylHb was generated by incubating Hb with a 10-fold molar excess of H_2O_2 over heme for 1 hour at 37°C. The ferryl ion is unstable and decomposes to different chemically heterogenous more stable oxidized Hb molecules. We use the term of ferrylHb to express the way of these molecules were formed rather than the real oxidation status of the heme iron. After oxidation, both metHb and ferrylHb were dialyzed against saline (3 times, 3h at 4°C) to remove excess $K_3Fe(CN)_6$ and H_2O_2. The purified Hb solutions were concentrated using Amicon Ultra centrifugal filter tubes (10,000 MWCO, Millipore Corp., Billerica, MA, USA). The purified and concentrated Hb stock solutions were aliquoted into single-use volumes, snap-frozen in liquid nitrogen, and stored at -70°C until used. The purity of Hb samples was evaluated by SDS-PAGE followed by silver staining, and the endotoxin content of Hb preparations was measured by Limulus amebocyte lysate assay (Lonza, Walkersville, MD, USA). The purity of Hb was above 99.9%.

Determination of Hb, metHb, ferrylHb, total and non-Hb-bound heme

In this work, we used two different spectrophotometric methods to calculate concentrations of Hb redox forms. For both methods, a full absorption spectrum between (250-700nm) of the samples was taken (NanoDrop 200, Thermo Fisher Scientific, MA, USA). We used the method of Winterbourn [144] to determine Hb, metHb, and hemichrome concentrations and used the recently published method of Meng and Alayash [145] to calculate Hb, metHb, and ferrylHb concentrations. All the equations used in the calculations of the different redox forms are listed in Table 2.

Table 2. Equations used in the calculations of the different redox forms

Calculations of Hb redox forms [mmol heme group/L]	Ref.
$[Hb] = -350.52\times OD_{541} + 388.95\times OD_{576} + 150.02\times OD_{630}$ $[metHb] = -185.77\times OD_{541} + 171.88\times OD_{576} + 387.58\times OD_{630}$ $[ferrylHb] = 702.23\times OD_{541} - 657.43\times OD_{576} - 455.64\times OD_{630}$	[145]
$[Hb] = 119\times OD_{576} - 39\times OD_{630} - 89\times OD_{560}$ $[metHb] = 28\times OD_{576} + 307\times OD_{630} - 55\times OD_{560}$ $[hemichrome] = -133\times OD_{576} - 114\times OD_{630} + 233\times OD_{560}$	[144]

Total heme content in plasma which is the sum of protein-bound and bioavailable heme was measured with QuantiChrom Heme Assay Kit (BioAssay Systems, Hayward, CA, USA) following the manufacturer's instructions. To determine non Hb-bound heme in plasma, we used the following equation: [non Hb-bound heme] = [total heme] − [Hb heme] − [metHb heme] − [hemichrome heme].

Kinetic measurements of ferrylHb formation

Purified Hb and metHb (60µmol/L heme group) were oxidized with various concentrations of H_2O_2 (125, 250, and 500 µmol/L) at 24°C. Absorption spectra were taken every minute after the addition of H_2O_2 for 10 minutes.

Mice

C57BL/6 (wild type, WT) and NLRP3 deficient ($NLRP3^{-/-}$) mice were maintained at the conventional experimental animal house at the University of Debrecen, with unrestricted access to water and food and environmental enrichment. The NLRP3 deficient mice were initially bred and characterized in the laboratory of J. Tschopp [100]. Sex and age-matched 6-8 weeks old mice were used in the experiments. All animal experiments were carried out with approval by the University of Debrecen Committee of Animal Welfare (Approval registration number: 2/2016/DEMÁB) followed the principles of the Basel Declaration and followed guidelines of the institutional and national ethical committee. The mice were euthanized by CO_2 inhalation and the blood was collected through heart puncture into heparin-coated tubes. To obtain plasma samples, the collected blood was centrifuged at 2000×*g*, 15 min, and 4°C. We perfused the mice with 5ml of sterile ice-cold phosphate-buffered saline (PBS) and thereafter collected the liver and spleen for further analysis.

Phenylhidrazine (PHZ)-induced intravascular hemolysis (IVH) mice model

To induce IVH, PHZ was administered intraperitoneally (i.p.). PHZ generates ROS, and PHZ-induced hemolysis is characterized by reduced RBC membrane deformability, spectrin

degradation, ATP depletion, lipid peroxidation, and cation imbalance [146-148]. We choose this IVH model because it is well-characterized, robust, and simple. To overwhelm the endogenous protective system against extracellular Hb and heme the mice received two injections of PHZ. First, 50 mg/kg body weight of PHZ (dissolved in sterile PBS up to a total volume of 200 µL) was injected then 16h later the second injection of PHZ was administered at the dosage of 30 mg/kg body weight. Control mice received sterile PBS. In the time-course experiments, the mice were sacrificed at 4, 16, and 20 hours after the first injection.

Hematocrit (Hct) measurement

K_3-EDTA-anticoagulated mouse whole blood samples were collected for full blood count and analyzed by Siemens Advia-2120i hematology analyzer (Tarrytown, NY, USA) with 800 Mouse C57BL program of Multi-Species software.

Mouse peritonitis model

Mouse peritonitis was induced in WT mice (n=25, male and female, 8-10 weeks old, 5 mice/group sex-matched) by intraperitoneal injection of heme, Hb, metHb, and ferrylHb (300 nmol heme/cavity) or LPS (100 µg/ cavity) in a volume of 200 µl using PBS as the vehicle. Control mice were injected with 200 µl of sterile PBS. Mice were euthanized by CO_2 exposure at 16 hours post-injection and infiltrated peritoneal leukocytes were collected by peritoneal lavage using 5 mL of ice-cold PBS containing 2% FCS (Gibco, Waltham, MA, USA). The collected cells were analyzed by flow cytometry (FACS Calibur, BD Biosciences). A fixed number of latex beads (Beckman Coulter, Paris, France) were used to determine the total number of cells collected. The number of peritoneal infiltrated neutrophils was determined by the use of R-phycoerythrin (R-PE)-conjugated rat anti-mouse Ly-6G (Gr1; CD11b, BD Biosciences, San Jose, CA) and biotin anti-mouse neutrophil monoclonal antibody (Clone 7/4, CL8993B, Cedarlane, Hornby, Ontario, Canada). Cells were co-stained with propidium iodide (0.5 µg/mL) to identify dead cells. Data were analyzed using FlowJo software (Tree Star, Inc. Ashland, OR). Ly- 6G and 7/4 double-positive cells were identified as neutrophils, Ly-6G negative, 7/4 positive cells were considered as inflammatory monocytes/macrophages [149].

Cell culture and treatment

Murine RAW 264.7 macrophage cell line was purchased from ATCC (Manassas, VA, USA). The RAW cells were cultured in supplemented DMEM (10% heat-inactivated fetal bovine serum (Gibco, Waltham, MA, USA), L-glutamine, and 1% penicillin/streptomycin) and incubated in 5% CO_2 humidified atmosphere at 37°C.

Primary mice bone marrow-derived macrophages (BMMs) were isolated from tibia and femur of 8-12 weeks old WT mice. Cells were flushed out from the bones under aseptic conditions with 10 mL of complete media. Cells were counted by a hemocytometer, re-suspended in complete medium supplemented with 50 ng/mL M-CSF (Miltenyi Biotec, Bergisch Gladbach, Germany), and seeded at a density of 3×10^5 cell/well in 96-well tissue culture plates. After 7 days the cultured BMMs differentiated and non-adherent cells were discarded. RAW and BMMs were primed with LPS (0111: B4 from Escherichia coli, 10 ng/mL) in complete DMEM containing 10% heat-inactivated FBS for 4h. Then LPS was removed and cells were treated with heme (25 μmol/L) and different Hb redox forms (25-150 μmol/L heme groups) in DMEM supplemented with 1% heat-inactivated FBS for a period specified at the particular experiments.

Cell viability assay

RAW cells were treated with different concentrations of heme (0-50 μmol/L) or Hb forms at the concentration of 250 μmol/L for 8h in DMEM 1% FBS. Following the treatment, cells were washed with sterile PBS then 100 μL of 3-[4,5-Dimethylthiazol-2-yl]-2,5-diphenyl-tetrazolium bromide (MTT, 0.5 mg/mL dissolved in HBSS) solution was added. After 4h of incubation, the MTT solution was removed and 100 μl of DMSO was added to dissolve the formazan crystals and the optical density of the wells was measured at 570 nm.

Quantitative real-time PCR (qRT-PCR)

We isolated RNA from the cells using TRizol (RNA-STAT60, Tel-Test Inc., Friendswood, TX, USA) according to the manufacturer's protocol. The cDNA was obtained by reverse transcribing of RNA by High- Capacity cDNA Reverse Transcription Kit (Applied Biosystems, Waltham, MA, USA). Quantitative RT-PCR was performed using iTaq Universal Probes Supermix (Bio-Rad Laboratories, Hercules, CA, USA) and predesigned primers and probes (TaqMan® Gene Expression Assays) to identify IL-1β (Mm 00434228), HO-1 (Mm 00516005) and GAPDH (Mm 99999915). GAPDH was used as an internal control gene to calculate relative gene expression with the delta-delta C_t ($\Delta\Delta C_t$) method.

Western blot

Liver samples were ground with liquid nitrogen and solubilized in lysis buffer to obtain the lysate for the investigation of caspase-1 activation and IL-1β processing. Twenty μg of protein were run on 12.5% SDS-PAGE at 100 V for and proteins were transferred to nitrocellulose membranes. Membranes were blocked with 6% dry milk in tris-buffered saline with tween 20

(TBS-T). Primary antibodies (polyclonal anti-caspase-1 p20 antibody (sc-398715, Santa Cruz Biotechnology Inc., Dallas, TX, USA), and a monoclonal anti-IL-1β antibody (12242, Cell Signaling Technology, Leiden, The Netherlands) in 1:1000 dilutions were incubated overnight at 4°C. Expression of HO-1 was evaluated both in the liver and whole cell lysate with the use of a polyclonal HO-1 antibody (ADI-SPA-896, Enzo Life Sciences Inc., Farmingdale, NY, USA). As secondary antibodies, horseradish peroxidase (HRP)-conjugated anti-rabbit and anti-mouse (NA931 and NA934 respectively, Amersham Biosciences Corp., Piscataway, NJ, USA) antibodies were used in 1:3000 dilutions. Antigen-antibody complexes were visualized with the HRP chemiluminescence system (Amersham Biosciences Corp., Piscataway, NJ, USA) and exposition of the membrane to X-ray films. Following detection, membranes were stripped and re-probed for β-actin using HRP-conjugated anti-β-actin antibody (sc-47778, Santa Cruz Biotechnology Inc., Dallas, TX, USA). Analysis and detection of Hb were done with the use of an HRP-conjugated polyclonal anti-Hb antibody (ab-19362, Abcam, Cambridge, UK). Band intensities on Western blots were quantified by Image Studio Digit Ver 5.2.

IL-1β secretion in macrophages

Secreted IL-1β was determined from cellular supernatant by ELISA analysis (DuoSet ELISA, R&D, Minneapolis, MN) according to the manufacturer's protocol.

Statistical analysis

Results are expressed as mean ± S.D. At least 3 independent experiments were performed for all *in vitro* studies. Statistical analyses were performed with GraphPad Prism software (version 8.01, San Diego, CA, USA). Comparisons between more than two groups were carried out by ordinary one-way ANOVA followed by post hoc Tukey's multiple-comparisons test. A value of $p < 0.05$ was considered significant.

RESULTS

1. Accumulation of extracellular heme forms in plasma after IVH

Massive destruction of RBCs in blood vessels is characterized by noticeable hemoglobinemia and in severe cases, high levels of bilirubin may be detected in the circulation [150]. To establish an IVH model, we injected WT mice with PHZ (50mg/kg bodyweight and 30mg/kg body weight 16h later, i.p.) while the control mice were injected with sterile PBS **(Fig. 6A)**. We collected the spleen and blood samples at all time points from both PHZ-treated and control mice. We observed brownish/yellowish discoloration of plasma at 4h post-PHZ injection which was intensified at 16h time point. As we expected, the spleen became darker and strikingly enlarged 20h post-injection **(Fig. 6A)**. Hematocrit levels decreased significantly at 4h after the first PHZ injection in comparison to PBS injected mice (0.5 ± 0.01 v/v% vs 0.36 ± 0.05 v/v%) and dropped further after the second injection (0.31 ± 0.01 v/v%) **(Fig. 6B)**. Next, we measured total heme levels in mice plasma following PHZ-induced IVH. We found a distinct increase of total heme 4 hours after the first PHZ injection (18.4 ± 1.6 µmol/L vs. 80.5 ± 16.9 µmol/L), and further increase up to 123.6 ± 16.4 µmol/L after the second PHZ injection at 16h time point (**Fig. 6C**).

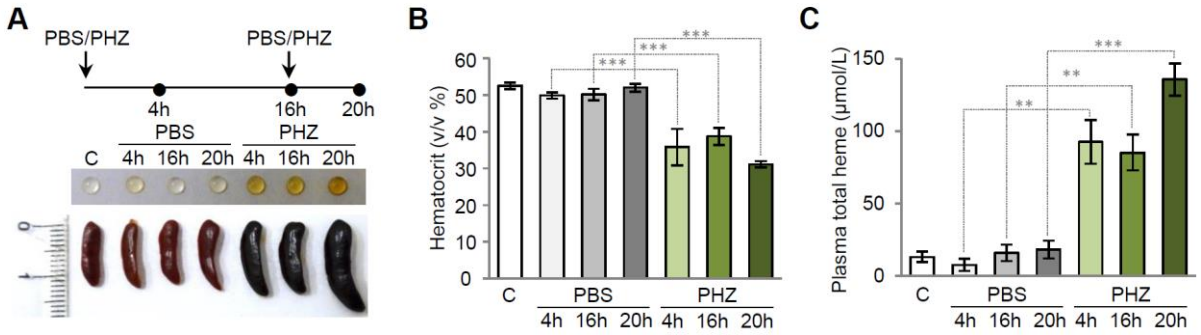

Figure 6. Intraperitoneal injection of PHZ induces hemolysis in mice. (A-C) C57BL/6 mice were injected with PHZ 50 mg/kg and 30 mg/kg 16 hrs later n=5, PBS (n=5) or left untreated. The mice were sacrificed at 4, 16 and 20 h time points. (A) Illustration of the experimental schedule and representative images of plasma and spleen samples derived from PHZ- or PBS-treated mice. (B) Hematocrit levels shown as mean ± S.D. measured from 5 biological replicates. (C) Plasma total heme levels shown as mean ± S.D. measured from 5 biological replicates. $^{**}p < 0.01$, $^{***}p < 0.005$.

Next, we determined the individual concentrations of the different Hb forms (Hb, metHb, and hemichrome), and calculated the amount of heme that has been released from Hb (non-Hb-bound heme) in the plasma samples of PHZ-, and vehicle-injected mice **(Fig. 7)**. Four hours after PHZ injection most of the heme was in the form of hemichromes (52.84 ± 6.9 µmol/L) and metHb (30.07 ± 6.44 µmol/L) while naïve Hb level was the lowest of the extracellular Hb forms **(Fig. 7A).** On the other hand, the level of non-Hb bound heme was very low (1.05 ± 0.56 µmol/L) **(Fig. 7B-D)**. Oxidized Hb forms remained the dominant forms at later time points as well, and the level of non-Hb bound heme increased significantly by the time in plasma of PHZ-injected mice **(Fig. 7B-D)**.

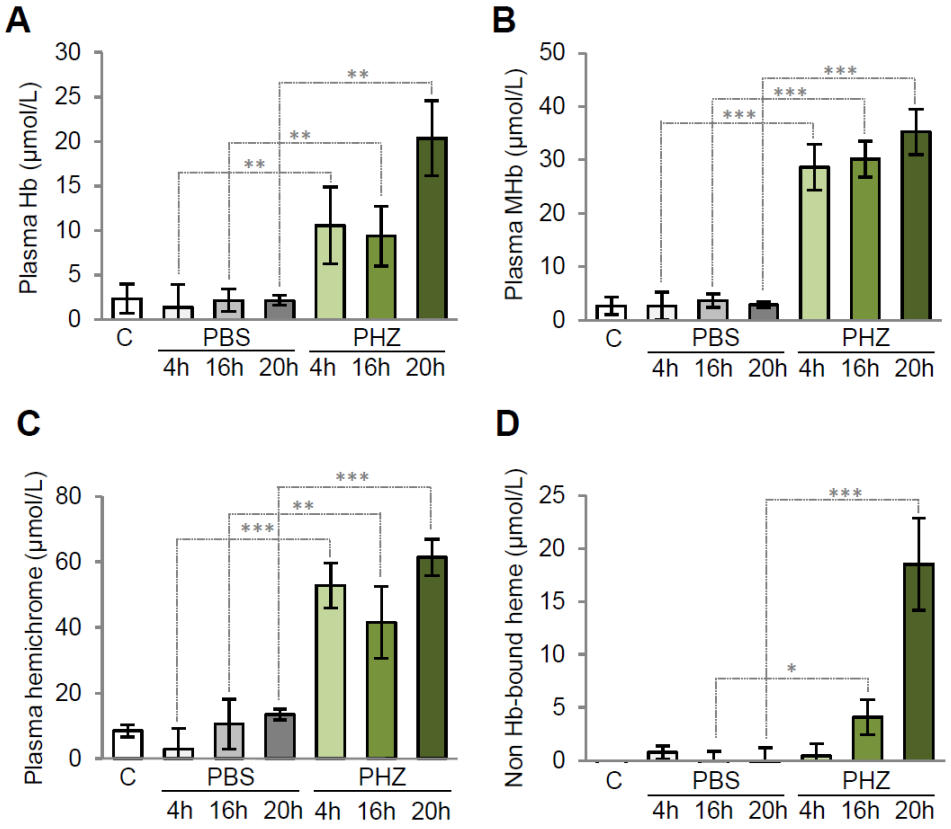

Figure 7. Intravascular hemolysis triggers the accumulation of cell free Hb, oxidation of Hb and heme release. C57BL/6 (WT) mice were injected (i.p) with PHZ 50mg/kg at 0h and 30mg/kg at 16h. (A) Total plasma heme upon IVH. (B) Hb, metHb (MHb), hemichrome and free heme were calculated in plasma at 4, 16 and 20 h time points after the injection. Free heme = [Total heme] - [Hb-bound heme]. *$p < 0.05$. **$p < 0.01$. ***$p < 0.005$.

2. IVH induces caspase-1 activation and mature IL-1β formation in mice liver

Heme triggers the release of IL-1β in macrophages through the activation of NLRP3 inflammasome as showed by Dutra et al. which mechanism is proposed to augment hemolysis-induced lethality in the mice [1]. To confirm this observation, we measured plasma levels of IL-1β in PHZ-injected mice. We found that PHZ injection triggered elevation of IL-1β plasma concentrations at 16h and 20h time points **(Fig. 8A)**. The majority of Hb is taken up and processed by the spleen and the liver upon intravascular hemolysis [18]. In line with this notion, we observed deep red discoloration of the liver in PHZ-treated mice that intensified at 20h. We analyzed the expression of HO-1, the enzyme responsible for heme degradation, and found that it was highly elevated in the liver of PHZ-injected mice at 16h post-injection **(Fig. 8B-C)**. We found a time-dependent increase of mature IL-1β levels in the liver of PHZ-injected mice compared to the control **(Fig. 8D)**. This increase was associated with time-dependent caspase-1 activation, suggesting the involvement of NLRP3 inflammasome activation in PHZ-induced production of IL-1β **(Fig. 8E)**.

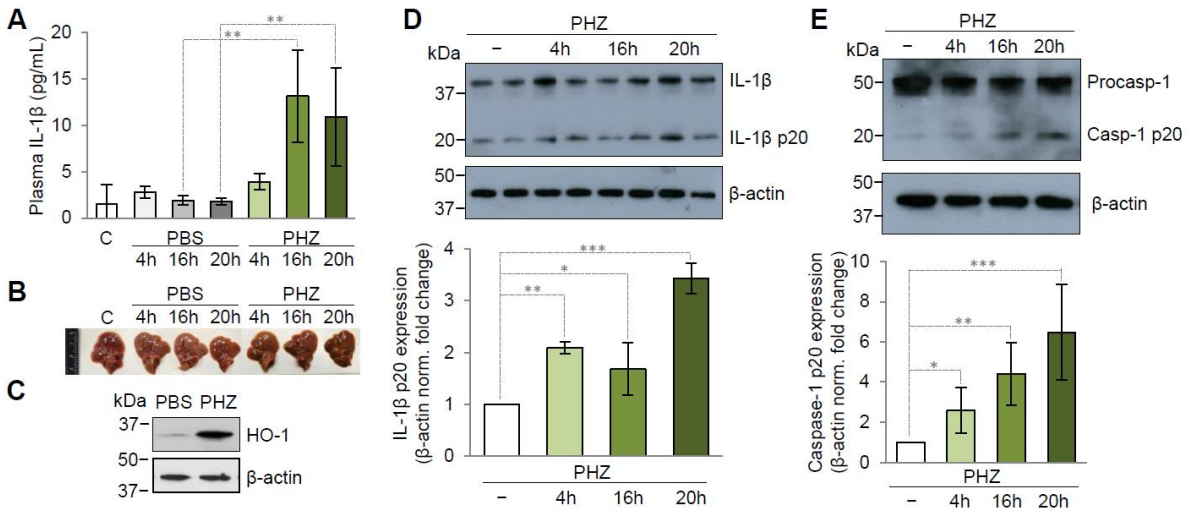

Figure 8. Intravascular hemolysis induces IL-1β production, HO-1 expression and caspase-1 activation. (A-D) C57BL/6 mice were treated (i.p.) with PHZ (n=5) or PBS (n=5) or left untreated (n=5). (A) IL-1β levels from plasma were determined by ELISA and are shown as mean ± S.D. (B) Representative images of liver are shown. (C-E) Protein expressions of HO-1 (16h), IL-1β and caspase-1 were analyzed by Western blot from liver samples at the indicated time points. Membranes were reprobed for β-actin. Representative blots of 3 independent experiments are shown. Densitometric analysis of Western blots is shown as mean ± S.D. of 3 independent experiments. *$p < 0.05$, **$p < 0.01$, ***$p < 0.005$.

3. Involvement of Hb forms with different redox states in IVH induced IL-1β formation

In our PHZ-induced hemolysis experiment, we observed that the majority of heme was present in the form of oxidized Hb forms and not in the form of free heme at the time of elevated production of IL-1β. This prompted us to postulate that these oxidized Hb forms play a role in the formation of IL-1β. To test this hypothesis, we obtained human blood from a healthy volunteer and prepared three Hb forms (Hb, metHb, and ferrylHb) with different oxidation states. Because under *in vitro* conditions NLRP3 inflammasome activation requires two distinct signals, we pretreated RAW264.7 murine macrophages with LPS (10 µg/mL, 24h). Then we treated the LPS-primed cells with the Hb forms of different oxidation states (25-150 µmol/L). We used heme at a concentration of 25 µmol/L as a positive control. In agreement with the previously reported effect [1], heme induced a pronounced increase of IL-1β mRNA and IL-1β processing in RAW264.7 macrophages **(Fig. 9A and B)**. Besides heme, all the Hb forms, upregulated IL-1β mRNA to a different extent in a concentration-dependent manner **(Fig. 9A)**, but only heme and ferrylHb induced the release of IL-1β to the cellular supernatant of LPS-primed RAW264.7 macrophages **(Fig. 9B)**.

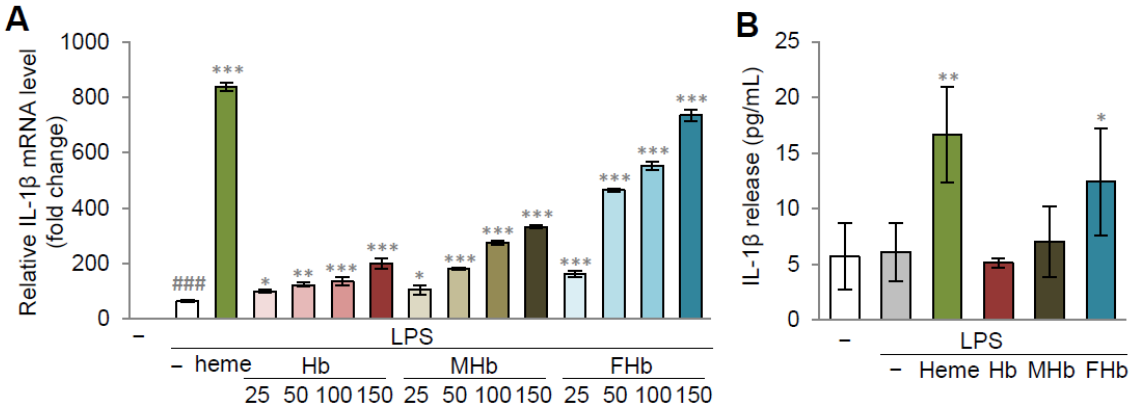

Figure 9. Induction of IL-1β mRNA and protein expressions in LPS-primed RAW264.7 macrophages by heme and Hb forms. (A-B) RAW264.7 cells were primed with LPS (10µg/mL, 24h) and exposed to heme (25 µmol/L) or Hb forms Hb, metHb (MHb) and ferrylHb (FHb) (25-150 µmol/L for mRNA, 150 µmol/L for protein). (A) IL-1β mRNA (4h) levels were determined by qRT-PCR. (B) IL-1β levels (6h) from cellular supernatant were determined by ELISA. Results are shown as mean ± S.D. from 3 independent experiments performed in triplicates. *$p < 0.05$, **$p < 0.01$, ***$p < 0.005$ as compared to LPS-treated control, $^{###}p < 0.005$ compared to no LPS treatment group.

To confirm these results, next we examined the effect of Hb forms on IL-1β secretion in LPS-primed bone marrow-derived macrophages (BMMs). Similarly to RAW264.7 macrophages heme and ferrylHb triggered IL-1β secretion in LPS-primed BMMs **(Fig. 10)**.

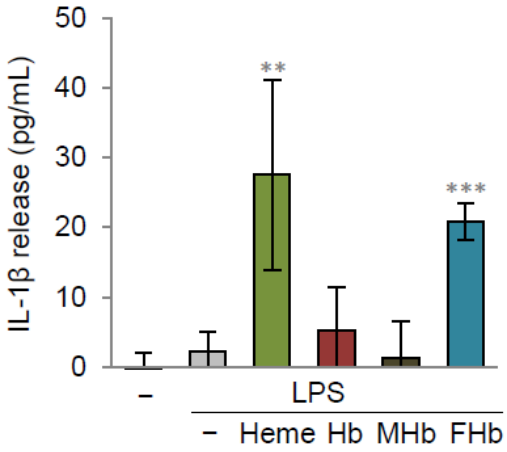

Figure 10. Induction of IL-1β secretion in LPS-primed BMMs by heme and Hb forms. BMMs were primed with LPS (10µg/mL, 24h) and exposed to heme (25 µmol/L) or Hb forms Hb, metHb (MHb) and ferrylHb (FHb), (150 µmol/L). IL-1β levels (6h) were determined by ELISA from cellular supernatant. Results are shown as mean ± S.D. from 3 independent experiments performed in triplicates. $^{**}p < 0.01$, $^{***}p < 0.005$.

LPS priming was necessary to trigger IL-1β production by heme and ferrylHb in both RAW264.7 cells and BMMs as non-primed cells failed to respond to heme or ferrylHb stimulation (data not shown).

4. Heme and oxidized Hb forms induce peritoneal infiltration of neutrophils and monocytes/macrophages

In the next experiment we investigated the pro-inflammatory effects of Hb forms *in vivo*, we injected heme and the Hb forms (300 nmol heme/cavity) into the peritoneal cavity of C57BL/6 mice. The peritoneal cavity was rinsed, neutrophil, and inflammatory monocytes/macrophage numbers were determined after 16 h of treatment. We found that heme and ferrylHb induced a remarkable intraperitoneal infiltration of neutrophils and monocytes **(Fig. 11 A-C)**. In contrast, metHb triggered only a mild elevation in the number of peritoneal neutrophils but did not induce monocyte recruitment, while Hb did not induce peritoneal infiltration of leukocytes at all **(Fig. 11 A-C)**.

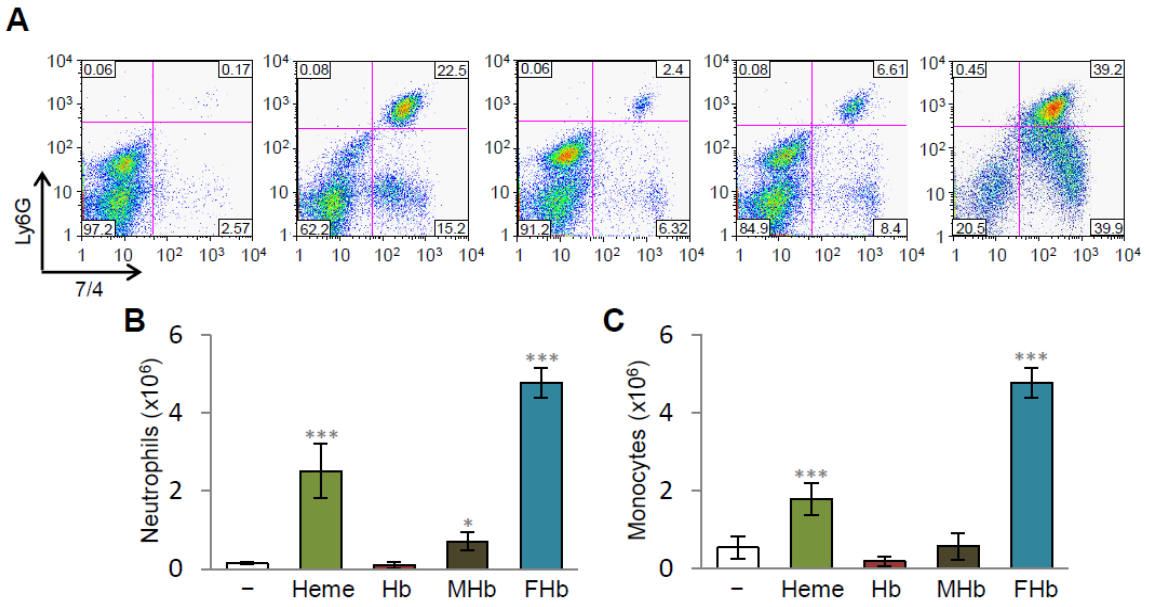

Figure 11. Induction of intraperitoneal leukocyte infiltration by heme and Hb forms in C57BL/6 mice. Heme and Hb forms Hb, metHb (MHb) and ferrylHb (FHb), (300 nmol heme/mice, n=5/group), or PBS (n=5) were injected into the peritoneal cavity of C57BL/6 mice. Peritoneal lavage was performed, neutrophil and inflammatory monocytes/macrophage numbers were determined after 16 h of treatment by flow cytometry. (A) Representative dot plots of peritoneal cells stained with Ly-6G and 7/4. (B) Mean number of Ly-6G high and 7/4 high PMN cells. (C) Mean number of Ly-6G low, 7/4 high inflammatory monocytes/macrophages. Data are presented as mean ± S.D. ***$p < 0.005$.

5. Heme and oxidized Hb forms induce caspase-1 activation and IL-1β processing in the liver of C57BL/6 mice

We have shown before that PHZ-induced hemolysis is associated with caspase-1 activation and IL-1β processing in the liver. Next, we investigated what Hb forms could be responsible for this effect. To this end, we injected heme and Hb forms (300 nmol heme/ mice) into the peritoneal cavity of C57BL/6 mice. We sacrificed the mice 16 hours after the treatments and analyzed caspase-1 and IL-1β protein expressions. We found that all the Hb forms as well as heme induced caspase-1 activation that was evidenced by the presence of the 20 kDa cleaved caspase-1 band (Casp-1 p20) **(Fig. 12A)**. Among the different heme sources, ferrylHb was the most potent inducer of caspase-1 activation, triggering an 8-fold elevation in the expression of Casp-1 p20 **(Fig. 12A)**. Alongside this observation, we detected a significantly increased level of active IL-1β (IL-1β p20) in the liver samples of ferrylHb and heme-treated mice (**Fig. 12B)**.

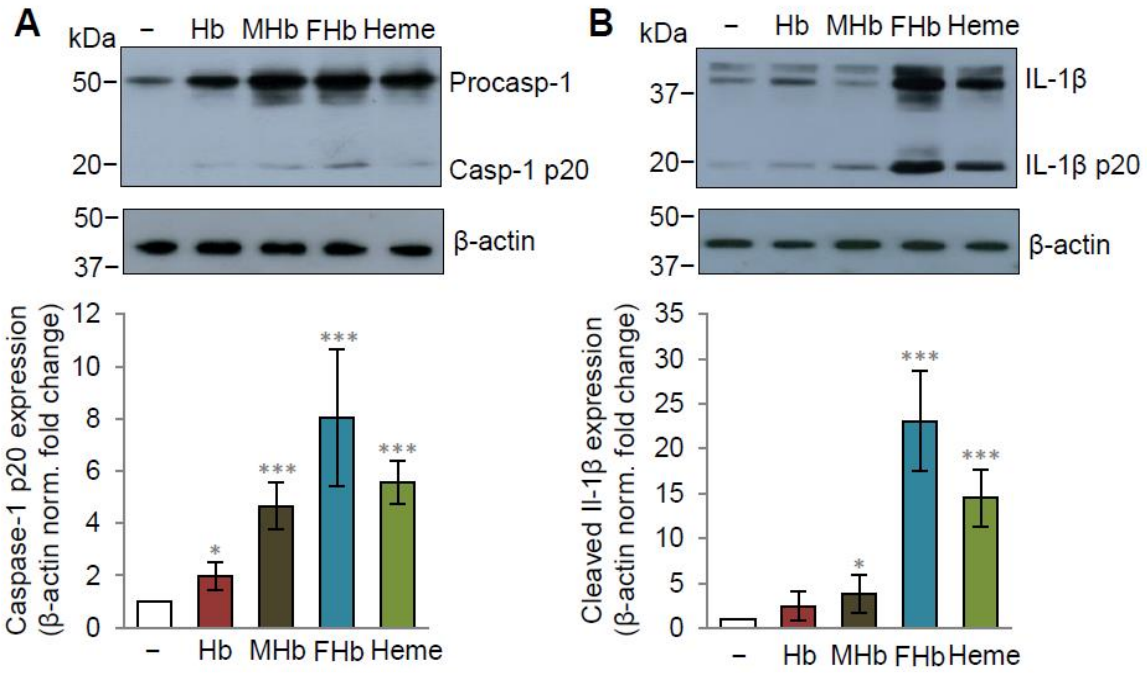

Figure 12. Induction of caspase-1 activation and IL-1β maturation in mouse liver by different heme forms. C57BL/6 mice were injected (i.p.) with heme or Hb forms Hb, metHb (MHb) and ferrylHb (FHb), (300 nmol heme/mice). Protein expressions of activated caspase-1 (Casp-1 p20) and processed IL-1β (IL-1β p20) were analyzed by Western blot from liver samples. Membranes were reprobed for β-actin. Representative blots of 3 independent experiments are shown. Densitometric analysis of Western blots is shown as mean ± S.D. of 3 independent experiments. *$p < 0.05$, **$p < 0.01$,***$p < 0.005$.

6. NLRP3 deficiency confers a survival advantage against IVH-mediated lethality

Severe IVH can be lethal such as we experienced in our PHZ-induced IVH model in C57BL/6 (WT) mice with 75% of lethality rate within 6 days after the first PHZ administration. To address the role of NLRP3 in severe hemolysis, we conducted a survival experiment in which we induced IVH with PHZ and compared survival rates of WT and NLRP3 deficient mice. Between days 2-6 after the first injection, 75% of WT mice died while 33% of PHZ injected NLRP3 deficient mice succumbed within the same period **(Fig. 13A)**. Then we wanted to know if PHZ treatment triggered the same degree of hemolysis in the WT and NLRP3$^{-/-}$ mice. First, we checked hematocrit levels 20 hours after the first PHZ injection, and we found no difference between WT and NLRP3$^{-/-}$ mice **(Fig. 13B)**. At the same time, there was no difference in the levels of plasma Hb, metHb, and hemichrome either **(Fig. 13C-E)**.

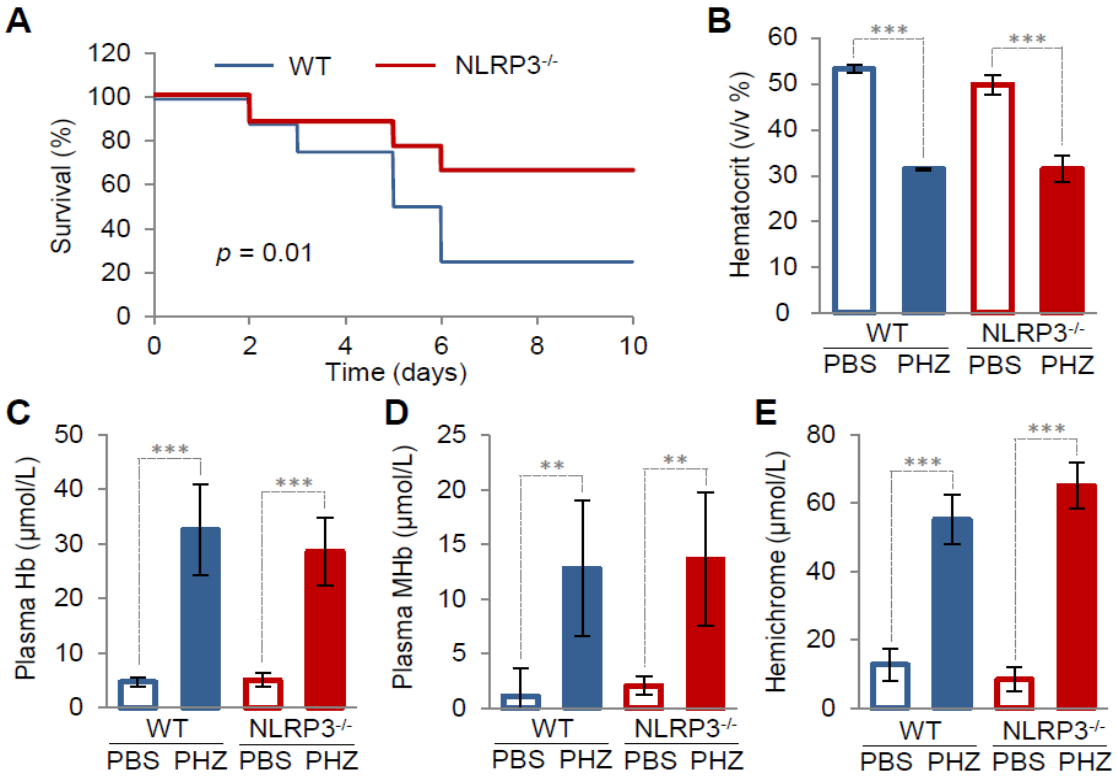

Figure 13. NLRP3 deficiency provides tolerance to mice against intravascular hemolysis-mediated lethality without impact on hemolysis. (A) C57BL/6 mice and NLRP3$^{-/-}$ mice were injected with PHZ (n=11/group), and survival was monitored for 10 days. (B-E) Plasma samples were collected 20 hours after PHZ or vehicle administration from WT (n=5/group) and Nlrp3$^{-/-}$ mice (n=5/group). Hematocrit (B), Hb (C), MHb (D) and hemichrome (E) levels were determined by spectral analysis. Data is presented as mean ± S.D. $^{**}p < 0.01$,$^{***}p < 0.005$.

7. NLRP3 plays a key role in hemolysis-associated IL-1β production

We established that IVH triggers IL-1β processing in the liver on WT mice. Next, we asked whether NLRP3 is involved in hemolysis-induced production of IL-1β. To this aim, we treated WT and NLRP3$^{-/-}$ mice with PHZ and investigated IL-1β processing in the liver. We found that while PHZ treatment induced an increase in the level of IL-1β p20 in WT mice, processing of IL-1β did not occur in PHZ-treated NLRP3$^{-/-}$ mice **(Fig. 14A)**. Similarly, the injection of ferrylHb failed to induce the formation of the processed IL-1β in the liver of NLRP3$^{-/-}$ mice **(Fig. 14B)**.

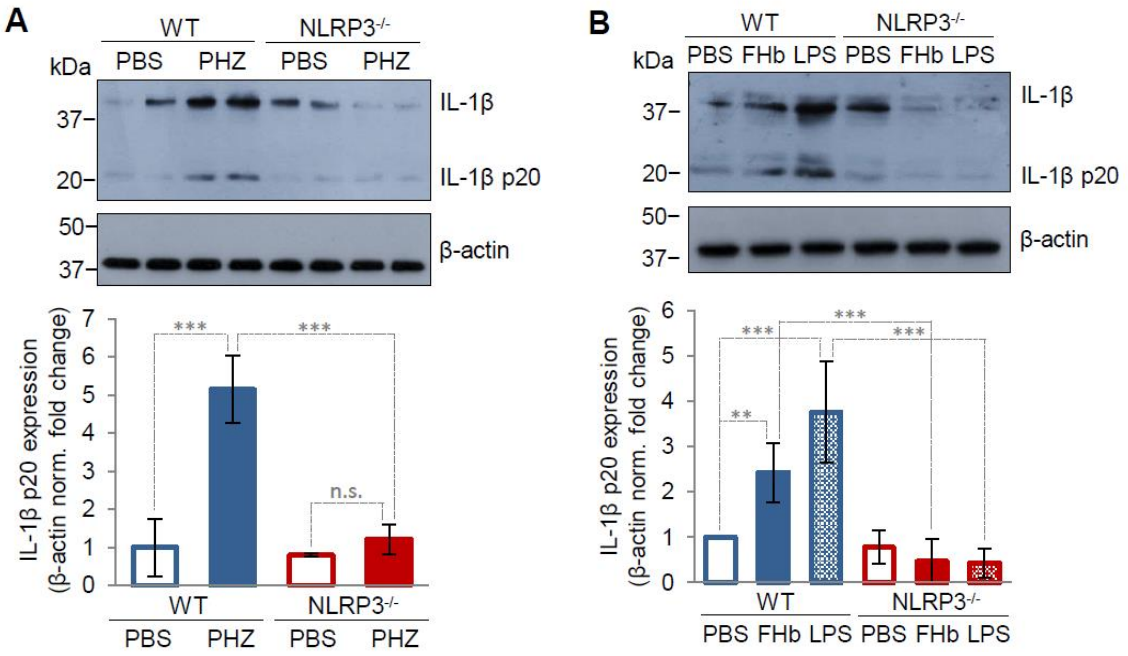

Figure 14. The critical role of NLRP3 in hemolysis-associated IL-1β processing
(A-B) WT and NLRP3$^{-/-}$ mice were injected with PHZ (50+30 mg/kg), ferrylHb (FHb, 300 nmol heme/peritoneal cavity), LPS (100 μg/peritoneal cavity) or PBS. Liver samples were collected at 20h time point and subjected to gel electrophoresis. Protein expression of IL-1β was analyzed by Western blot. Band intensity of IL-1β p20 was normalized to β-actin. Representative blots of 3 independent experiments are shown. Densitometric analysis of Western blots is shown as mean ± S.D. of 3 experiments. $^{**}p < 0.01$, $^{***}p < 0.005$.

8. Difficulties of the detection of ferrylHb in biological samples

To calculate the plasma concentrations of the different Hb forms we used the method of Winterbourn which allowed us to calculate Hb, metHb, and hemichrome concentrations, but not the ferryl form. On the other hand, we detected covalently crosslinked Hb dimers in the plasma and urine samples obtained from PHZ-treated mice **(Fig. 15A-D)**. We assumed that these Hb dimers are the product of intermolecular electron transport between ferryl ion and the susceptible amino acid of the globin chains and subsequent reaction between the formed globin radicals. Therefore we wanted to detect ferrylHb in the plasma samples of PHZ-treated mice with a recently published spectrophotometric method of Meng and Alayash [145].

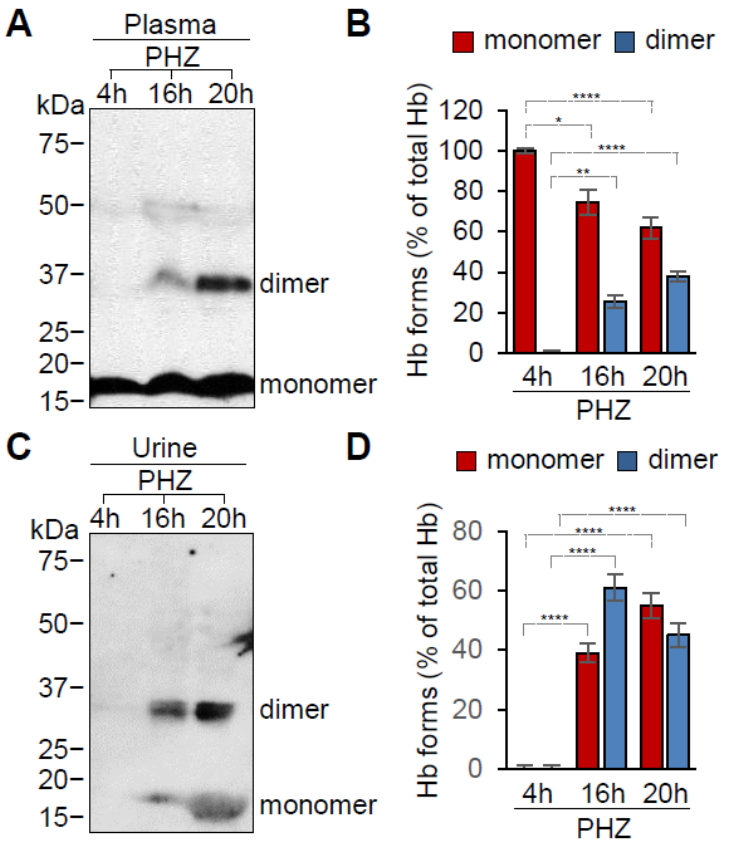

Figure 15. Accumulation of covalently crosslinked Hb dimers in plasma and urine upon IVH. (A-D) Plasma and urine samples were collected from C57BL/6 mice (n=5/group) following PHZ injection at the indicated time points. (A and C) Representative Hb western blots and (B and D) densitometric analysis are presented. Bars show mean ± S.D. P values were calculated using one-way ANOVA followed by Tukey's multiple comparison analysis. *$p < 0.05$, **$p < 0.01$, ****$p < 0.001$.

9. Kinetics and H_2O_2 concentration-dependence of ferrylHb formation, decomposition and crosslinked Hb formation *in vitro*

Interestingly, we could not detect ferrylHb in either plasma or urine samples obtained from PHZ-injected mice. To understand this discrepancy we analyzed the formation of ferrylHb and covalently crosslinked Hb forms *in vitro*. To this end, we reacted Hb and metHb with H_2O_2 that triggers a 2-electron oxidation of heme iron and measured the concentrations of Hb, metHb, and ferrylHb. When we reacted Hb (50 µmol/L) with different concentrations of H_2O_2 (125-500 µmol/L) for 10 minutes we observed a dose-dependent formation of metHb, and as expected, a decline in Hb concentration **(Fig. 16A)**. We observed a low amount of ferrylHb formation only when Hb was reacted with high concentrations of H_2O_2 (>250 µmol/L) **(Fig.**

16A). When we reacted metHb with H_2O_2 (125-500 µmol/L, 10 min) we detected ferrylHb (Fig. 2B) at all concentrations, but paradoxically ferrylHb formation inversely correlated with the concentration of H_2O_2 **(Fig. 16B)**.

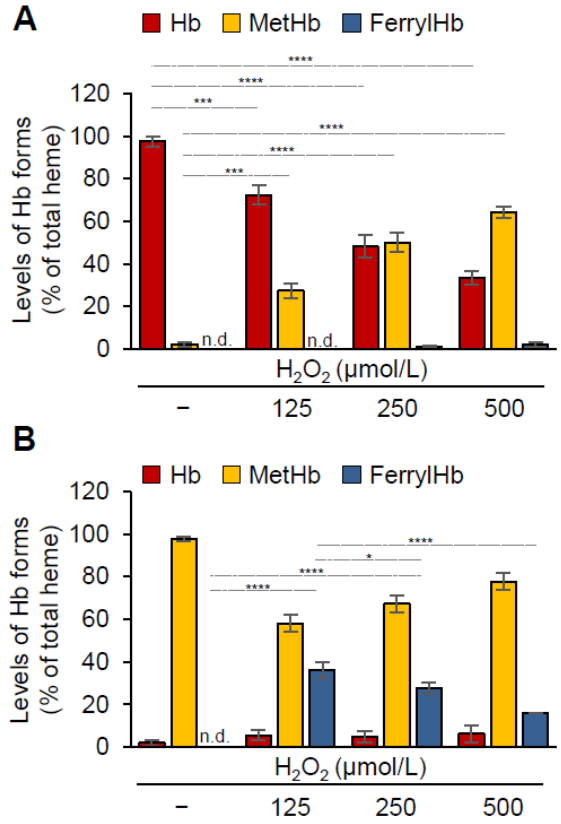

Figure 16. Formation of ferrylHb in hydrogen peroxide-induced oxidation of Hb and metHb. (A) Human Hb and (B) metHb (60 µmol/L heme) were oxidized with H_2O_2 (125, 250 and 500 µmol/L) for 10 minutes at 37°C. Concentrations of different redox states of Hb were determined and the presence of different Hb forms as a percentage of total heme was calculated. Bar graph shows mean ± S.D. from 3 independent experiments. P values were calculated using one-way ANOVA followed by Tukey's multiple comparison analysis. *p < 0.05, ***p < 0.005, ****p < 0.001.

It is known that the ferryl oxidation state is highly unstable and stabilizes via intramolecular electron transfer between the iron ion and the globin chains which leads eventually to the formation of covalent bonds between the Hb subunits [151, 152]. Therefore, next, we addressed whether this crosslinked Hb formation occurred in our *in vitro* reactions. We subjected the samples generated in the reactions between Hb and metHb with H_2O_2 to denaturing SDS-PAGE and detected Hb by Western blot. We found a dose-dependent formation of Hb dimers in the reaction between Hb and H_2O_2 **(Fig. 17A and B)**. We observed a more pronounced formation of Hb dimers and the formation of Hb tetramers in the reaction between metHb. Moreover, we found a more pronounced Hb dimer formation in the reaction between metHb and H_2O_2 than in the reaction between Hb and H_2O_2 **(Fig. 17A and B)**.

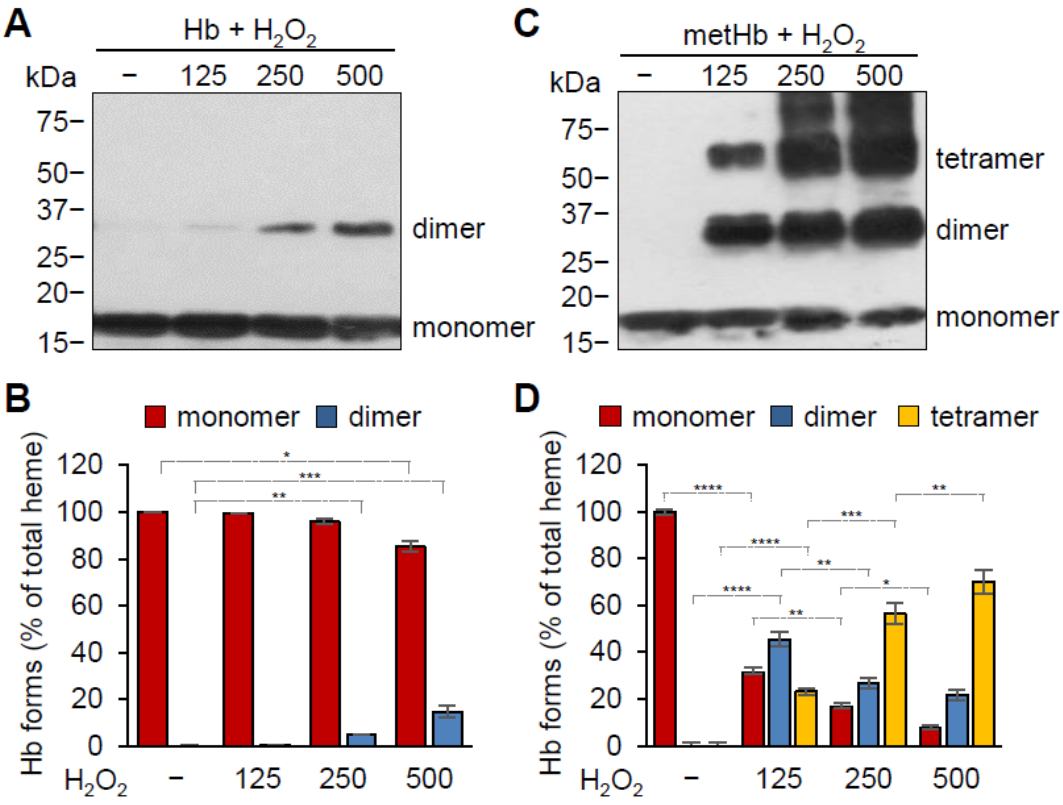

Figure 17. Formation of Hb multimers in hydrogen peroxide-induced oxidation of Hb and metHb. Purified Hb and metHb (60 µmol/L heme) was reacted with different concentrations of H_2O_2 (125, 250 and 500 µmol/L) for 30 minutes at 37°C. (A and C) Representative western blots after (A) Hb and (C) metHb oxidation. (B and D) Densitometric analysis of western blots and the percentages of gmoxHb multimers as a percent of total Hb. Bar graph shows mean ± S.D. from 3 independent experiments. P values were calculated using one-way ANOVA followed by Tukey's multiple comparison analysis. *$p < 0.05$, **$p < 0.01$, ***$p < 0.005$.

Using similar experimental settings, next, we investigated the kinetics of ferrylHb production and decomposition in the reaction between metHb and different concentrations of H_2O_2 (125-500 µmol/L). We took the absorption spectra of the samples in every minute for 10 minutes and calculated the concentrations of the different Hb redox forms. We found that the ferrylHb level peaked at around 2 minutes after the initiation of the reaction and then declined at each H_2O_2 concentrations **(Fig. 18A)**. We observed that the peak level of ferrylHb (~45% of total Hb) was independent of H_2O_2 concentration **(Fig. 18A)**. On the contrary, the rate of ferrylHb decomposition was dose-dependent. At the highest concentration of H_2O_2 (500 µmol/L) we detected the fastest rate of ferryHb decomposition (1.72 ± 0.17 µmol/L ferrylHb/min) **(Fig. 18B)**. Concentrations of metHb and ferrylHb changed the exact opposite directions in the course of the reaction between metHb and H_2O_2 **(Fig. 18C)**. Finally, we investigated how the

dose of H_2O_2 and the time influence the formation of covalently cross-linked Hb forms. We observed that H_2O_2 dose-dependently induced the formation of Hb dimers within 1 minute **(Fig. 18D and E)**. Furthermore, 250 and 500 µmol/L H_2O_2 induced the formation of Hb tetramers within 10 minutes dose-dependently **(Fig. 18D and E)**.

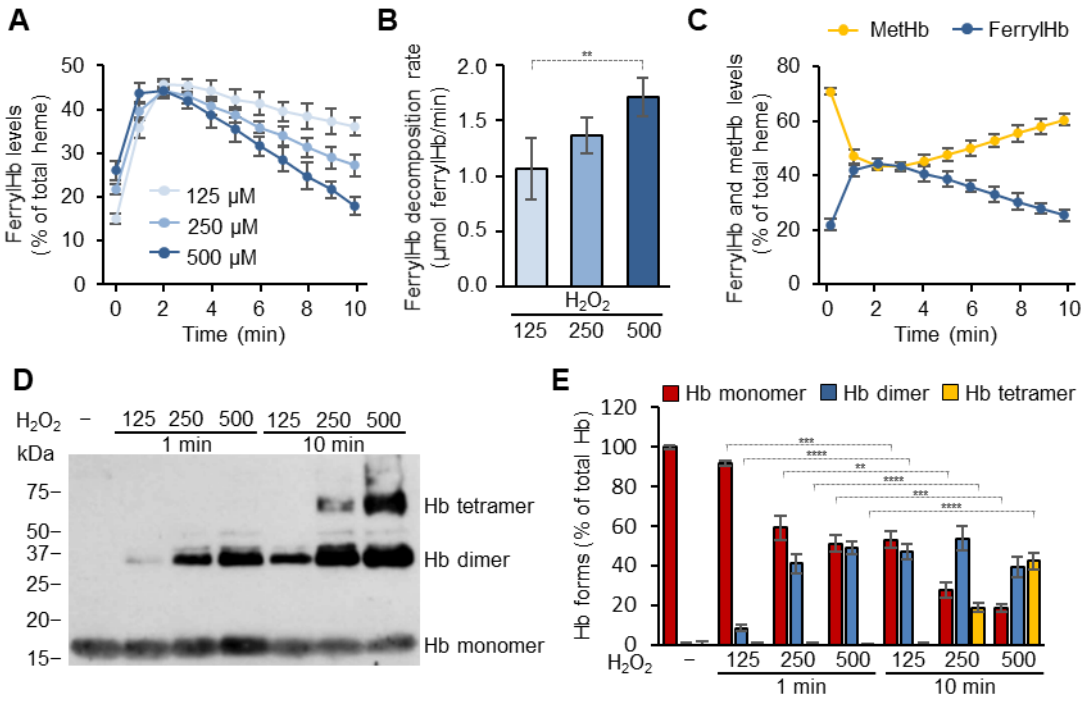

Figure 18. Decay of ferrylHb leads to the regeneration of metHb and formation of Hb multimers. (A-C) Purified human metHb (60 µmol/L heme) was oxidized with H_2O_2 (125, 250 and 500 µmol/L) and the concentrations of Hb forms were determined every minute for 10 minutes. (A) Time-, and dose-dependent formation and decomposition of ferrylHb in the reaction between metHb and H_2O_2 presented as mean ± S.D. of 3 independent experiments. (B) FerrylHb decomposition rate (µmol ferrylHb/min) was calculated at each H_2O_2 concentration from the kinetic measurements. Graph shows mean ± S.D. of 3 independent experiments. (C) Time-dependent changes of ferrylHb and metHb levels in the course of metHb oxidation with H_2O_2 (500 µmol/L) presented as mean ± S.D. of 3 independent experiments. (D-E) Time-, and dose-dependent formation of Hb multimers in the course of metHb oxidation with H_2O_2. (D) Representative western blot is shown. (E) Densitometric analysis of western blots was performed and the percentages of Hb monomers, dimers and tetramers as a percent of total Hb were calculated. Bar graph shows mean ± S.D. from 3 independent experiments. P values were calculated using one-way ANOVA followed by Tukey's multiple comparison analysis. $^{**}p < 0.01$, $^{***}p < 0.005$, $^{****}p < 0.001$.

DISCUSSION

DAMPs are endogenous molecules that originate from damaged cells and tissues with the ability to trigger and/or modify innate immune responses. Upon hemolysis, Hb is released from RBCs to the circulation and give a rise to the production of different Hb redox states and heme which can act as DAMPs. Heme is the best characterized Hb-derived DAMP that targets different immune and non-immune cells. Heme is a chemoattractant, activates the complement system, modulates host defense mechanisms through the activation of innate immune receptors and the heme oxygenase-1/ferritin system, and induces innate immune memory **(Fig. 19)**.

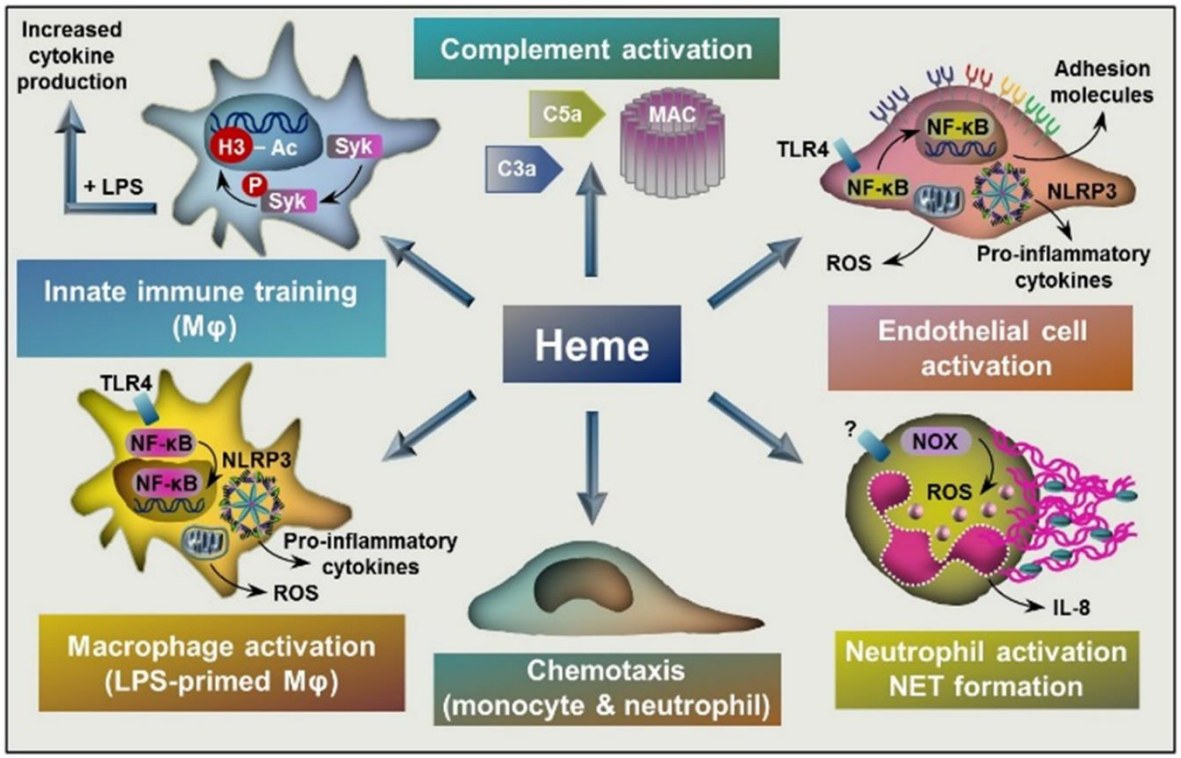

Figure 19. Targets of extracellular heme. Labile heme induces endothelial cell activation characterized by NF-κB activation, elevated ROS production and increased expression of adhesion molecules and pro-inflammatory cytokines. Heme activates neutrophils characterized by elevated ROS production through the activation of NOX, increased production of IL-8 and NET formation. Heme induces monocyte and neutrophil chemotaxis. Labile heme induces ROS production, NLRP3 activation and proinflammatory cytokine production in LPS-primed macrophages. Heme induces innate immune training through triggering epigenetic changes, such as acetylation of H3 at lysine-27 in monocytes and macrophages in a Syk-dependent manner. Heme induces complement activation leading to the formation of C3a and C5a activation fragments and the assembly of MAC. Abbreviations: NF-κB: nuclear factor kappa B; ROS: reactive oxygen species; NOX: NADPH oxidase; NET: neutrophil extracellular trap; TLR4: toll-like receptor 4, NLRP3: NLR family pyrin domain containing 3; LPS: lipopolysaccharide; Syk: Spleen tyrosine kinase; H3: histone 3, MAC: membrane attack complex.

On the other hand, it is still unclear whether upstream hemolysis-derived products contribute to the detrimental effects of massive hemolysis. In fact, in a recent study of Merle et al. showed that IVH-induced renal alterations are largely heme-independent, since the administration of free heme cannot mimic them, and scavenging heme could not prevent them [143]. Our aim in this work was to provide a detailed analysis of extracellular heme forms following IVH and to investigate the contributions of these heme forms to hemolysis-associated inflammation, particularly NLRP3 inflammasome activation and subsequent production of IL-1β.

We injected PHZ intraperitoneally to induce IVH in mice. We choose this IVH model because it is well-characterized, robust, and simple. Because we wanted to study the pro-inflammatory properties of the heme forms produced upon IVH, it was necessary to induce hemolysis in a sterile way. Splenomegaly is a well-known characteristic feature of massive IVH [70], that we also experienced in the PHZ-treated mice together with decreased hematocrit levels, which is a widely used clinical marker of RBC volume in the blood [153]. We found high amounts of extracellular heme in the plasma in PHZ-injected mice that together with the decreased hematocrit level suggested that RBC lysis occurred, as we expected, in the PHZ-injected mice. In a recent study Gouveia et. al detected similar amounts of heme in mice plasma after PHZ injection using a different assay to determine heme [154].

Analysis of the plasma heme forms revealed that 4 hours after PHZ-injection the largest portion of plasma heme was present in hemichromes. Extensive hemichrome formation during PHZ-induced IVH is known and is attributed to the strong oxidative effect of PHZ [155]. MetHb was the second most abundant form of heme in plasma samples obtained 4 hours after the PHZ injection. Although it is known that metHb readily releases its heme prosthetic group [61], we could not detect non-Hb-bound heme in the plasma of PHZ-injected mice at this time-point. We assume that at this time-point the heme scavenging capacity of plasma of PHZ-injected was not overwhelmed, and the released heme was rapidly cleared from the circulation by Hx. On the contrary, after two doses of PHZ, at 20h time-point we detected a considerable amount of labile heme (~20 μmol/L) in the plasma. Accumulation of plasma heme starts after the depletion Hb and heme scavenging proteins [154], therefore we assume that by this time point Hp and Hx were depleted from the circulation. Recently Gouveia et al. developed a cell-based heme reporter assay with the use of a heme-specific single domain antibody [154]. Using that sophisticated method they reported that the amount of bioavailable heme is around 2-5 μmol/L in the plasma of PHZ-treated mice [154] which is around one-tenth to one-fifth that we have measured. Besides Hx, plasma contains several non-specific heme-binding proteins such as albumin, and lipoproteins such as LDL and HDL can bind heme as well [63, 156]. We

assume that most of the non-Hb-bound heme we detected in the plasma of PHZ-treated mice was associated with non-specific heme-binding proteins or transferred to hydrophobic lipid compartments, whereas the method of Gouveia et al. measured exclusively the amount of free heme. Additionally, we used low centrifugal force for plasma separation, which may have left RBC-derived microparticles in the plasma and could have influenced our heme measurement. Studies show that these microparticles are bioactive and contribute to the pathogenesis of sickle cell disease and the formation of RBC storage lesions [139, 140, 157].

Growing evidence suggests that extracellular Hb and free heme are harmful, explaining the existence of the defense mechanisms that control their deleterious effects. On the other hand, in the case of massive IVH, this protective system can be overwhelmed, and Hb and its oxidation products can accumulate in the plasma. Most studies examined the pro-oxidant and pro-inflammatory properties of heme. For instance, studies show that heme elicits a pro-inflammatory response in leukocytes and endothelial cells through the activation of pattern recognition receptors such as TLR4 or NLRP3 [53, 118, 123, 158, 159]. Studies generally applied high concentrations of free heme (up to 100 μmol/L), although there was always a lot of argument regarding the amount of bioavailable heme under certain pathological conditions. Recent evidence suggests that the amount of heme is much lower than it was assumed previously [154].

A recent study suggested that IVH-induced organ damage is mostly heme independent, and evidence is gaining about the pro-inflammatory actions of upstream hemolysis-derived products. For example, Silva et al. showed that ferrylHb induces endothelial cell activation characterized by elevated expression of vascular adhesion molecules, and impairs endothelial barrier function through reorganization of the actin cytoskeleton [56]. In this work we detected caspase-1 activation and the formation of active IL-1β in the liver and increased levels of IL-1β in the plasma of PHZ-treated mice as compared to control, suggesting that acute hemolysis triggers a systemic inflammatory response.

Previously Dutra et al. identified heme as a trigger of NLRP3 inflammasome activation and IL-1β production in a PHZ-induced IVH model [1]. Mononuclear cells are likely to be a source of pro-inflammatory cytokines such as IL-1β, and heme was shown to induce IL-1β production in LPS-primed macrophages [1]. Interestingly, we found that the increase in IL-1β plasma levels precedes the accumulation of non-Hb bound heme in the plasma, therefore we tested the different Hb forms upstream of free heme whether they are involved in the inflammatory response triggered by IVH.

We purified Hb from human blood and oxidized it into metHb and ferrylHb and investigated their pro-inflammatory activity under *in vitro* conditions. Here we have to note that we use the term ferrylHb to define an Hb form that was extensively oxidized with H_2O_2, but because of the reactive nature of ferryl ion, this preparation is a mixture of the products of ferrylHb decomposition. We found that besides heme, ferrylHb also induces upregulation and the release of IL-1β in both RAW cells and BMMs. On the contrary, Hb and metHb failed to induce IL-1β secretion.

Heme and ferrylHb treatment triggered IL-1β release only when the macrophages were primed with LPS before heme and ferrylHb challenge. This observation is in agreement with the established mechanism of inflammasome activation in the literature, based on the fact that NLRP3 inflammasome activation and active IL-1β formation requires two distinct signals [160]. In our *in vitro* experimental settings, priming of macrophage with LPS served as a first signal while heme or ferrylHb was the second signal. Nevertheless, the injection of PHZ to the mice without prior LPS treatment triggered the release of IL-1β in the livers and plasma in our experimental system. We assume that gut-derived LPS may have served as a first signal under the *in vivo* conditions since severe hemolysis could potentially disrupt intestinal epithelial barrier consequently amplifying gut permeability [161, 162]. Further studies may be necessary to establish this mechanism in the PHZ-induced intravascular hemolysis model.

To further examine the pro-inflammatory potential of the different Hb forms we investigated whether they induce peritonitis in mice. We found that ferrylHb and to a lesser extent heme, but not Hb or metHb induced infiltration of monocytes into the peritoneal cavity. Previously liver seemed to be a good target organ to investigate PHZ-induced caspase-1 activation and active IL-1β formation, therefore we used the same approach to further explore the pro-inflammatory effect of the different Hb forms *in vivo*. Intraperitoneal administration of ferrylHb and heme but not Hb and metHb induced caspase-1 activation and processing of IL-1β.

Heme-globin interaction is weakened in oxidized Hb forms therefore they can release heme. Heme released from metHb and ferrylHb is bioavailable and can trigger for example oxidative modification of LDL, or induce HO-1 expression in endothelial cells [163-165]. Because heme and ferrylHb exhibit similar pro-inflammatory potential in these experimental settings one can assume that ferrylHb-mediated pro-inflammatory response is mediated by the released heme. We would argue with this assumption. Previously Kassa et al. determined the kinetics of heme release from different oxidized Hb forms using heme scavenging proteins and lung epithelial cells as reporter systems [61]. They demonstrated that metHb releases heme at

a considerably higher rate and triggers higher expressions of HO-1 in lung alveolar epithelial cells than ferrylHb [61]. Combining these results with our observations we assume that the pro-inflammatory effect of ferrylHb is independent of heme release because if the response would have been mediated by the released heme, metHb should have triggered the same or stronger responses than ferrylHb.

Cellular stress and infections activate innate immune receptors such as NLRP1, NLRP3, NLRC4, or AIM2 to form a molecular platform, inflammasome, to facilitate the activation of pro-inflammatory caspase-1 and subsequent maturation and release of IL-1β [166-169]. Previous studies showed that among these immune receptors, the NLRP3 inflammasome drives heme-mediated IL-1β production in macrophages as well as in endothelial cells [1, 124, 170]. Moreover, Dutra et al. showed that mice deficient of NLRP3 inflammasome components such as apoptosis-associated speck-like protein containing caspase activation and recruitment domain (ASC), caspase-1 or NLRP3 itself are tolerant to intravascular hemolysis-induced lethality as compared to wild type mice [1].

In this work, we confirmed that NLRP3 deficiency confers a survival advantage to mice in PHZ-induced severe IVH. The survival advantage of $NLRP3^{-/-}$ deficient mice can rely on two different mechanisms. It can be associated with increased resistance of $NLRP3^{-/-}$ mice to PHZ-induced RBC lysis, or it can be the result of increased tolerance of $NLRP3^{-/-}$ mice to severe IVH. We found no differences in either hematocrit levels or the concentrations of Hb forms between WT and $NLRP3^{-/-}$ mice which results ruled out the possibility of increased resistance of $NLRP3^{-/-}$ mice to PHZ-induced RBC lysis.

Growing evidence suggests that controlling tissue damage in the host upon infection or sterile inflammation can largely improve the survival chances of the host. The importance of this so-called disease tolerance in influencing host survival has been proved in diverse disease models [171]. Our results revealed that neither PHZ nor ferrylHb induced active IL-1β formation in $NLRP3^{-/-}$ mice which most likely contributed to their survival advantage upon severe IVH.

In this work, we identified ferrylHb as a potent pro-inflammatory oxidized Hb form that induces the production of active IL-1β. On the other hand, detection of ferrylHb is difficult due to its high reactivity, and for a long time, we were lacking a simple method to measure its concentration. Recently Meng and Alayash developed a spectrophotometric method to measure ferrylHb [145]. Still, we could not detect ferrylHb, but we detected covalently crosslinked Hb dimers in the plasma as well as in urine samples obtained from PHZ-treated mice. We assumed that covalently crosslinked Hb dimers formed during the stabilization of the ferryl ion. To

further investigate this, we used an *in vitro* approach and investigated the kinetics of the formation of ferrylHb and the covalently crosslinked Hb forms in the course of H_2O_2-induced Hb and metHb oxidation. The reaction between metHb H_2O_2 yielded more ferrylHb than the reaction between Hb and H_2O_2. Interestingly, we found that the formation of ferrylHb was inversely proportional to the concentration of H_2O_2. Further studying the reaction between metHb and H_2O_2 revealed that ferrylHb concentration reaches its maximum at around two minutes after initiation of the reaction followed by a decomposition of ferrylHb which rate was dependent on the concentration of H_2O_2.

It is established in the literature that ferrylHb decomposes through intermolecular electron transfer between ferryl iron and specific amino acid residue of globin subunit leading to the formation of ferric iron and globin-centered radicals [54, 80, 81, 172]. The reaction between globin-globin radicals produces covalently cross-linked Hb multimers [10]. Along with these notions, we showed an inverse relationship between the concentrations of metHb and ferrylHb during the reaction of metHb and H_2O_2 and we detected the formation of covalently cross-linked Hb multimers in a time- and dose-dependent manner.

These covalently cross-linked Hb multimers lack a precise name unanimously agreed among the scientific community. It should be noted that the two-electron oxidation of Hb or metHb ultimately forms the cross-linked Hb multimers. The oxidation state of heme iron in these Hb forms is +3 (ferric) a reason why in much of the literature these forms are referred to as metHb. We are convinced that this is a misnomer because the nomenclature ignores the modification of the globin subunit which gives this form of Hb unique features. In other studies, the authors refer to this form as ferryHb which is a misleading name for this Hb form as well because the ferryl oxidation state is transitory. Therefore, we proposed to name the Hb forms produced in the two-electron oxidation of Hb or metHb as globin modified oxidized Hb (gmoxHb). We believe that a unique name will help to distinguish these species from metHb (ferric Hb without globin modification) as well as from ferrylHb (unstable redox form of Hb).

Taken together we demonstrated that following intravascular hemolysis different Hb oxidation products are formed which we assume to contribute to sterile hemolysis-induced inflammatory reactions. We proposed the name of gmoxHb for the oxidized Hb form that is produced via ferrylHb formation. We showed that Western blot is the appropriate tool for detecting gmoxHb in biological samples. We identified gmoxHb as a potent pro-inflammatory trigger that induces formation and maturation of IL-1β both *in vitro* and *in vivo*. The gmoxHb-mediated inflammatory response is mediated through NLRP3 inflammasome activation and caspase-1 activation.

Further work needs to be done to clarify the role of gmoxHb in the pathogenesis of hemolytic diseases, and because gmoxHb is a heterogeneous entity, to identify the most dangerous species among the Hb crosslinks with different sizes and structures.

SUMMARY

Labile heme is a prototypical DAMP that plays a critical role in hemolysis-associated inflammation and organ damage. On the other hand, a recent study provided evidence that IVH-induced renal damage could not be prevented by Hx therapy and could not be mimicked by heme administration. This finding suggests that heme might not be the ultimate DAMP upon IVH and postulates that upstream hemolysis-derived products may contribute to the detrimental effects of massive hemolysis. In this work, we demonstrated that following intravascular hemolysis Hb oxidation occurs leading to the formation of metHb, hemichromes, covalently crosslinked Hb multimers, and eventually free heme. We showed that PHZ-induced IVH triggers IL-1β production which response is mediated through NLRP3 inflammasome activation. We provided evidence that covalently crosslinked Hb forms were produced during the decomposition of the highly reactive ferrylHb. We proposed the name of gmoxHb for the oxidized Hb form that is produced via ferrylHb formation. We identified gmoxHb as a potent pro-inflammatory Hb form which induces active IL-1β production both *in vitro* and *in vivo*. We confirmed that NLRP3 deficiency confers a survival advantage to mice in PHZ-induced IVH via increased tolerance and improved tissue damage control mechanisms. Growing evidence support the pathophysiological role of innate immune system activation in diverse pathologies associated with IVH. Thus, identification of RBC-derived DAMPs and understanding the signaling mechanisms affected by them might provide new approaches for treating pathological conditions with IVH.

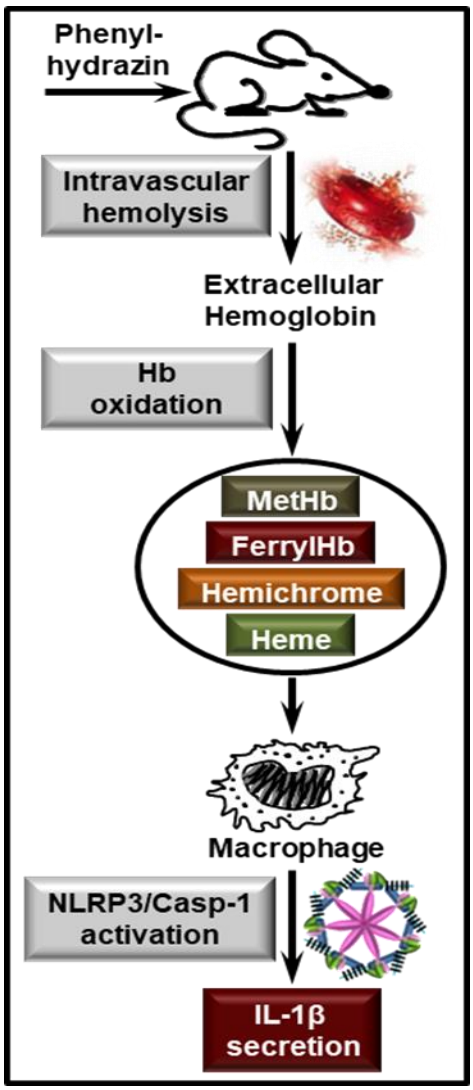

Figure 19. Proposed model of IVH-associated production of IL-1β. Administration of PHZ induces IVH in mice. Hb is accumulated and oxidation occurs. Targeting macrophages oxidized Hb forms induce NLRP3 and caspase-1 activation, leading to the cleavage of pro-IL-1β and the secretion of the active cytokine.

KEYWORDS

- red blood cells
- intravascular hemolysis
- damage-associated molecular patterns (DAMPs)
- hemoglobin
- hemoglobin oxidation
- heme
- NLRP3 inflammasome activation
- IL-1β
- ferryl hemoglobin
- covalently crosslinked hemoglobin multimers

LIST OF ABBREVIATIONS

ASC: apoptosis-associated speck-like protein containing a caspase recruitment domain

ATP: adenosine triphosphate

BMMs: bone marrow-derived macrophages

BR: bilirubin

BV: biliverdin

BVR: biliverdin reductase

CD163: cluster of differentiation 163

CO: carbon monoxide

DAMP: damage-associated molecular pattern

DEAE: diethyl-amino-ethyl

DMEM: Dulbecco's Modified Eagle's medium

FBS: fetal bovine serum

FerrylHb: ferryl hemoglobin

FLVCR1a and FLVCR1b: feline leukemia virus subgroup receptors 1a and 1b

FtH and FtL: ferritin Heavy chain and ferritin light chain

GAPDH: Glyceraldehyde 3-phosphate dehydrogenase

GmoxHb: globin modified oxidized hemoglobin

Gpx: glutathione peroxidase

H_2O_2: hydrogen peroxide

Hb: hemoglobin

HbA: adult hemoglobin

HbF: fetal hemoglobin

HBSS: Hank’s balanced salt solution

HO-1: heme oxygenase-1

Hp: haptoglobin

HRP: horseradish peroxidase

HUVEC: human umbilical vein endothelial cell

Hx: hemopexin

ICAM-1: intercellular adhesion molecule-1

IL-1β: interleukin 1 beta

IVH: intravascular hemolysis

$K_3Fe(CN)_6$: potassium ferricyanide

kDa: kilodalton

LDL: low-density lipoprotein

LPS: lipopolysaccharide

LRR: leucine reach repeat

M-CSF: macrophage Colony Stimulating Factor

metHb: methemoglobin

MP: microparticle

MTT: 3-[4,5-Dimethylthiazol-2-yl]-2,5-diphenyl-tetrazolium bromide

NAC: N-acetyl cysteine

NF-κB: nuclear factor kappa B

NLRP3: NOD-like receptor family, pyrin domain containing 3

NLR: NOD-like receptor

OD: optical density

P2X7: P2X purinoceptor 7

PAMPs: pathogen-associated molecular patterns

PBS: phosphate-buffered saline

PHZ: phenylhydrazine

PPIX: protoporphyrin IX

Prdx 1 and Prdx 2: peroxiredoxin 1 and peroxiredoxin 2

PRRs: pathogen recognition receptors

RBCs: red blood cells

ROS: reactive oxygen species

SDS-PAGE: sodium dodecyl sulfate-polyacrylamide gel electrophoresis

SOD: superoxide dismutase

ST2: suppression of tumorigenesis 2

Syk: spleen tyrosine kinase

TBS-T: tris buffered saline with Tween 20

TFR1: transferrin receptor 1

TIR: Toll/IL-1 receptor

TLR4: toll-like receptor 4

TNF: tumor necrosis factor

TNFR1: tumor necrosis factor receptor 1

TLR: toll-like receptor

VCAM-1: vascular cell adhesion molecule-1

WT: wild type

ACKNOWLEDGEMENT

I am immensely grateful to my supervisor Dr. Viktoria Jeney for the professional guidance she has offered me throughout this work. Her dedication, the vast subject knowledge, and leadership skills ever challenged and motivated me over the years I have been under her supervision. Her keenness and wit in the day to day work helped me to cultivate critical thinking and problem-solving skill. I will always cherish her relentless effort to ensure the wellbeing of our group even outside the lab. Thank you very much.

I would like to extend my gratitude to Prof. József Tőzsér as the head of doctoral school and Prof. Zoltán Papp as the head of the Research Centre for Molecular Medicine for their support to our group.

Very special thanks to my colleagues Judit Erdei, Andrea Tóth, and Enikő Balogh for the technical help they have persistently given me and their cooperation in the day to day errands of the lab. I greatly value their effort to ensure a good working environment for everyone.

Last, in order but not of importance, I would like to thank my family and friend for the emotional support they have given me. I always drew strength from them to pull me through the difficult times.

REFERENCES

1. Dutra, F.F., et al., *Hemolysis-induced lethality involves inflammasome activation by heme.* Proc Natl Acad Sci U S A, 2014. **111**(39): p. E4110-8.
2. Gozzelino, R., V. Jeney, and M.P. Soares, *Mechanisms of Cell Protection by Heme Oxygenase-1.* Annual Review of Pharmacology and Toxicology, 2010. **50**: p. 323-354.
3. Dzierzak, E. and S. Philipsen, *Erythropoiesis: development and differentiation.* Cold Spring Harb Perspect Med, 2013. **3**(4): p. a011601.
4. Muckenthaler, M.U., et al., *A Red Carpet for Iron Metabolism.* Cell, 2017. **168**(3): p. 344-361.
5. Gell, D.A., *Structure and function of haemoglobins.* Blood Cells Mol Dis, 2018. **70**: p. 13-42.
6. Ratanasopa, K., et al., *Dissection of the radical reactions linked to fetal hemoglobin reveals enhanced pseudoperoxidase activity.* Front Physiol, 2015. **6**: p. 39.
7. Perutz, M.F., *Structure of hemoglobin.* Brookhaven Symp Biol, 1960. **13**: p. 165-83.
8. Baldwin, J.M., *Structure and function of haemoglobin.* Prog Biophys Mol Biol, 1975. **29**(3): p. 225-320.
9. Siems, W.G., O. Sommerburg, and T. Grune, *Erythrocyte free radical and energy metabolism.* Clin Nephrol, 2000. **53**(1 Suppl): p. S9-17.
10. Jeney, V., et al., *Natural history of the bruise: formation, elimination, and biological effects of oxidized hemoglobin.* Oxidative medicine and cellular longevity, 2013. **2013**: p. 703571.
11. Iuchi, Y., et al., *Elevated oxidative stress in erythrocytes due to a SOD1 deficiency causes anaemia and triggers autoantibody production.* Biochemical Journal, 2007. **402**: p. 219-227.
12. Neumann, C.A., et al., *Essential role for the peroxiredoxin Prdx1 in erythrocyte antioxidant defence and tumour suppression.* Nature, 2003. **424**(6948): p. 561-565.
13. Lee, T.H., et al., *Peroxiredoxin II is essential for sustaining life span of erythrocytes in mice.* Blood, 2003. **101**(12): p. 5033-5038.
14. Ho, Y.S., et al., *Mice deficient in cellular glutathione peroxidase develop normally and show no increased sensitivity to hyperoxia.* J Biol Chem, 1997. **272**(26): p. 16644-51.
15. Percy, M.J., N.V. McFerran, and T.R. Lappin, *Disorders of oxidised haemoglobin.* Blood Rev, 2005. **19**(2): p. 61-8.
16. Balagopalakrishna, C., et al., *Superoxide produced in the heme pocket of the beta-chain of hemoglobin reacts with the beta-93 cysteine to produce a thiyl radical.* Biochemistry, 1998. **37**(38): p. 13194-202.
17. Vitturi, D.A., et al., *Antioxidant functions for the hemoglobin beta 93 cysteine residue in erythrocytes and in the vascular compartment in vivo.* Free Radical Biology and Medicine, 2013. **55**: p. 119-129.
18. de Back, D.Z., et al., *Of macrophages and red blood cells; a complex love story.* Front Physiol, 2014. **5**: p. 9.
19. Piomelli, S. and C. Seaman, *Mechanism of Red-Blood-Cell Aging - Relationship of Cell-Density and Cell Age.* American Journal of Hematology, 1993. **42**(1): p. 46-52.
20. Franco, R.S., *The measurement and importance of red cell survival.* American Journal of Hematology, 2009. **84**(2): p. 109-114.
21. Bratosin, D., et al., *Cellular and molecular mechanisms of senescent erythrocyte phagocytosis by macrophages. A review.* Biochimie, 1998. **80**(2): p. 173-195.
22. Khandelwal, S., N. van Rooijen, and R.K. Saxena, *Reduced expression of CD47 during murine red blood cell (RBC) senescence and its role in RBC clearance from the circulation.* Transfusion, 2007. **47**(9): p. 1725-1732.
23. Lutz, H.U., *Innate immune and non-immune mediators of erythrocyte clearance.* Cell Mol Biol (Noisy-le-grand), 2004. **50**(2): p. 107-16.

24. Arese, P., F. Turrini, and E. Schwarzer, *Band 3/complement-mediated recognition and removal of normally senescent and pathological human erythrocytes.* Cell Physiol Biochem, 2005. **16**(4-6): p. 133-46.
25. Kay, M.M., *Band 3 and its alterations in health and disease.* Cell Mol Biol (Noisy-le-grand), 2004. **50**(2): p. 117-38.
26. Lutz, H.U., M. Nater, and P. Stammler, *Naturally-Occurring Anti-Band-3 Antibodies Have a Unique Affinity for C3.* Immunology, 1993. **80**(2): p. 191-196.
27. Fernandez-Boyanapalli, R.F., et al., *Impaired apoptotic cell clearance in CGD due to altered macrophage programming is reversed by phosphatidylserine-dependent production of IL-4.* Blood, 2009. **113**(9): p. 2047-2055.
28. Boas, F.E., L. Forman, and E. Beutler, *Phosphatidylserine exposure and red cell viability in red cell aging and in hemolytic anemia.* Proceedings of the National Academy of Sciences of the United States of America, 1998. **95**(6): p. 3077-3081.
29. Kobayashi, N., et al., *TIM-1 and TIM-4 glycoproteins bind phosphatidylserine and mediate uptake of apoptotic cells.* Immunity, 2007. **27**(6): p. 927-940.
30. Park, S.Y., et al., *Rapid cell corpse clearance by stabilin-2, a membrane phosphatidylserine receptor.* Cell Death and Differentiation, 2008. **15**(1): p. 192-201.
31. White, C., et al., *HRG1 Is Essential for Heme Transport from the Phagolysosome of Macrophages during Erythrophagocytosis.* Cell Metabolism, 2013. **17**(2): p. 261-270.
32. Meynard, D., J.L. Babitt, and H.Y. Lin, *The liver: conductor of systemic iron balance.* Blood, 2014. **123**(2): p. 168-76.
33. Maines, M.D., *The heme oxygenase system: a regulator of second messenger gases.* Annu Rev Pharmacol Toxicol, 1997. **37**: p. 517-54.
34. Harrison, P.M. and P. Arosio, *The ferritins: molecular properties, iron storage function and cellular regulation.* Biochim Biophys Acta, 1996. **1275**(3): p. 161-203.
35. Knutson, M.D., et al., *Iron loading and erythrophagocytosis increase ferroportin 1 (FPN1) expression in J774 macrophages.* Blood, 2003. **102**(12): p. 4191-7.
36. Nemeth, E., et al., *Hepcidin regulates cellular iron efflux by binding to ferroportin and inducing its internalization.* Science, 2004. **306**(5704): p. 2090-3.
37. Ohgami, R.S., et al., *Identification of a ferrireductase required for efficient transferrin-dependent iron uptake in erythroid cells.* Nat Genet, 2005. **37**(11): p. 1264-9.
38. Schultz, I.J., et al., *Iron and Porphyrin Trafficking in Heme Biogenesis.* Journal of Biological Chemistry, 2010. **285**(35): p. 26753-26759.
39. Shaw, G.C., et al., *Mitoferrin is essential for erythroid iron assimilation.* Nature, 2006. **440**(7080): p. 96-100.
40. Chiabrando, D., et al., *The mitochondrial heme exporter FLVCR1b mediates erythroid differentiation.* Journal of Clinical Investigation, 2012. **122**(12): p. 4569-4579.
41. Schaison, G., *[Sickle cell anemia, an example of a constitutional disease of hemoglobin].* Rev Stomatol Chir Maxillofac, 1983. **84**(3): p. 144-8.
42. Bossi, D. and M. Russo, *Hemolytic anemias due to disorders of red cell membrane skeleton.* Molecular Aspects of Medicine, 1996. **17**(2): p. 171-188.
43. van Wijk, R. and W.W. van Solinge, *The energy-less red blood cell is lost: erythrocyte enzyme abnormalities of glycolysis.* Blood, 2005. **106**(13): p. 4034-4042.
44. Zanella, A. and P. Bianchi, *Red cell pyruvate kinase deficiency: from genetics to clinical manifestations.* Baillieres Best Pract Res Clin Haematol, 2000. **13**(1): p. 57-81.
45. Garratty, G. and L.D. Petz, *Drug-Induced Immune Hemolytic-Anemia.* American Journal of Medicine, 1975. **58**(3): p. 398-407.
46. Berentsen, S., U. Randen, and G.E. Tjonnfjord, *Cold agglutinin-mediated autoimmune hemolytic anemia.* Hematol Oncol Clin North Am, 2015. **29**(3): p. 455-71.
47. Lippi, G. and F. Sanchis-Gomar, *Epidemiological, biological and clinical update on exercise-induced hemolysis.* Ann Transl Med, 2019. **7**(12): p. 270.

48. Deplaine, G., et al., *The sensing of poorly deformable red blood cells by the human spleen can be mimicked in vitro.* Blood, 2011. **117**(8): p. e88-95.
49. Mebius, R.E. and G. Kraal, *Structure and function of the spleen.* Nat Rev Immunol, 2005. **5**(8): p. 606-16.
50. Rifkind, J.M., J.G. Mohanty, and E. Nagababu, *The pathophysiology of extracellular hemoglobin associated with enhanced oxidative reactions.* Front Physiol, 2014. **5**: p. 500.
51. Fortes, G.B., et al., *Heme induces programmed necrosis on macrophages through autocrine TNF and ROS production.* Blood, 2012. **119**(10): p. 2368-2375.
52. Wagener, F.A., et al., *Heme-induced cell adhesion in the pathogenesis of sickle-cell disease and inflammation.* Trends Pharmacol Sci, 2001. **22**(2): p. 52-4.
53. Porto, B.N., et al., *Heme induces neutrophil migration and reactive oxygen species generation through signaling pathways characteristic of chemotactic receptors.* Journal of Biological Chemistry, 2007. **282**(33): p. 24430-24436.
54. Jia, Y., et al., *Structural basis of peroxide-mediated changes in human hemoglobin: a novel oxidative pathway.* The Journal of biological chemistry, 2007. **282**(7): p. 4894-907.
55. Schaer, D.J., et al., *CD163 is the macrophage scavenger receptor for native and chemically modified hemoglobins in the absence of haptoglobin.* Blood, 2006. **107**(1): p. 373-80.
56. Silva, G., et al., *Oxidized hemoglobin is an endogenous proinflammatory agonist that targets vascular endothelial cells.* J Biol Chem, 2009. **284**(43): p. 29582-95.
57. Melamed-Frank, M., et al., *Structure-function analysis of the antioxidant properties of haptoglobin.* Blood, 2001. **98**(13): p. 3693-3698.
58. Wicher, K.B. and E. Fries, *Evolutionary aspects of hemoglobin scavengers.* Antioxid Redox Signal, 2010. **12**(2): p. 249-59.
59. Kristiansen, M., et al., *Identification of the haemoglobin scavenger receptor.* Nature, 2001. **409**(6817): p. 198-201.
60. Rother, R.P., et al., *The clinical sequelae of intravascular hemolysis and extracellular plasma hemoglobin - A novel mechanism of human disease.* Jama-Journal of the American Medical Association, 2005. **293**(13): p. 1653-1662.
61. Kassa, T., et al., *Differential heme release from various hemoglobin redox states and the upregulation of cellular heme oxygenase-1.* Febs Open Bio, 2016. **6**(9): p. 876-884.
62. Allhorn, M., et al., *Processing of the lipocalin alpha(1)-microglobulin by hemoglobin induces heme-binding and heme-degradation properties.* Blood, 2002. **99**(6): p. 1894-1901.
63. Fasano, M., et al., *Heme binding to albuminoid proteins is the result of recent evolution.* Iubmb Life, 2007. **59**(7): p. 436-440.
64. Miller, Y.I. and N. Shaklai, *Kinetics of hemin distribution in plasma reveals its role in lipoprotein oxidation.* Biochimica Et Biophysica Acta-Molecular Basis of Disease, 1999. **1454**(2): p. 153-164.
65. Paoli, M., et al., *Crystal structure of hemopexin reveals a novel high-affinity heme site formed between two beta-propeller domains.* Nature Structural Biology, 1999. **6**(10): p. 926-931.
66. Alam, J. and A. Smith, *Receptor-Mediated Transport of Heme by Hemopexin Regulates Gene-Expression in Mammalian-Cells.* Journal of Biological Chemistry, 1989. **264**(30): p. 17637-17640.
67. Eskew, J.D., et al., *Cellular protection mechanisms against extracellular heme - Heme-hemopexin, but not free heme, activates the N-terminal c-Jun kinase.* Journal of Biological Chemistry, 1999. **274**(2): p. 638-648.
68. Hvidberg, V., et al., *Identification of the receptor scavenging hemopexin-heme complexes.* Blood, 2005. **106**(7): p. 2572-9.
69. Tolosano, E., et al., *Defective recovery and severe renal damage after acute hemolysis in hemopexin-deficient mice.* Blood, 1999. **94**(11): p. 3906-3914.

70. Tolosano, E., et al., *Enhanced splenomegaly and severe liver inflammation in haptoglobin/hemopexin double-null mice after acute hemolysis.* Blood, 2002. **100**(12): p. 4201-4208.
71. Tenhunen, R., H.S. Marver, and R. Schmid, *The enzymatic conversion of heme to bilirubin by microsomal heme oxygenase.* Proc Natl Acad Sci U S A, 1968. **61**(2): p. 748-55.
72. Maines, M.D., *Heme Oxygenase - Function, Multiplicity, Regulatory Mechanisms, and Clinical-Applications.* Faseb Journal, 1988. **2**(10): p. 2557-2568.
73. Kapitulnik, J. and M.D. Maines, *Pleiotropic functions of biliverdin reductase: cellular signaling and generation of cytoprotective and cytotoxic bilirubin.* Trends Pharmacol Sci, 2009. **30**(3): p. 129-37.
74. Piantadosi, C.A., *Carbon monoxide, reactive oxygen signaling, and oxidative stress.* Free Radic Biol Med, 2008. **45**(5): p. 562-9.
75. Stocker, R., et al., *Bilirubin Is an Antioxidant of Possible Physiological Importance.* Science, 1987. **235**(4792): p. 1043-1046.
76. Motterlini, R. and R. Foresti, *Biological signaling by carbon monoxide and carbon monoxide-releasing molecules.* American Journal of Physiology-Cell Physiology, 2017. **312**(3): p. C302-C313.
77. Arosio, P., L. Elia, and M. Poli, *Ferritin, Cellular Iron Storage and Regulation.* Iubmb Life, 2017. **69**(6): p. 414-422.
78. Harel, S. and J. Kanner, *The Generation of Ferryl or Hydroxyl Radicals during Interaction of Hemoproteins with Hydrogen-Peroxide.* Free Radical Research Communications, 1988. **5**(1): p. 21-33.
79. Svistunenko, D.A., et al., *The globin-based free radical of ferryl hemoglobin is detected in normal human blood.* Journal of Biological Chemistry, 1997. **272**(11): p. 7114-7121.
80. Deterding, L.J., et al., *Identification of free radicals on hemoglobin from its self-peroxidation using mass spectrometry and immuno-spin trapping - Observation of a histidinyl radical.* Journal of Biological Chemistry, 2004. **279**(12): p. 11600-11607.
81. Ramirez, D.C., Y.R. Chen, and R.P. Mason, *Immunochemical detection of hemoglobin-derived radicals formed by reaction with hydrogen peroxide: involvement of a protein-tyrosyl radical.* Free radical biology & medicine, 2003. **34**(7): p. 830-9.
82. Riccio, A., et al., *The crystal structure of a tetrameric hemoglobin in a partial hemichrome state.* Proceedings of the National Academy of Sciences of the United States of America, 2002. **99**(15): p. 9801-9806.
83. Vollaard, N.B.J., et al., *A new sensitive assay reveals that hemoglobin is oxidatively modified in vivo.* Free Radical Biology and Medicine, 2005. **39**(9): p. 1216-1228.
84. Reeder, B.J., et al., *Toxicity of myoglobin and haemoglobin: oxidative stress in patients with rhabdomyolysis and subarachnoid haemorrhage.* Biochem Soc Trans, 2002. **30**(4): p. 745-8.
85. Nagy, E., et al., *Red Cells, Hemoglobin, Heme, Iron, and Atherogenesis.* Arteriosclerosis Thrombosis and Vascular Biology, 2010. **30**(7): p. 1347-U190.
86. Crist, E. and A.I. Tauber, *Selfhood, immunity, and the biological imagination: The thought of Frank Macfarlane Burnet.* Biology & Philosophy, 2000. **15**(4): p. 509-533.
87. Matzinger, P., *Essay 1: The danger model in its historical context.* Scandinavian Journal of Immunology, 2001. **54**(1-2): p. 4-9.
88. Matzinger, P., *Tolerance, Danger, and the Extended Family.* Annual Review of Immunology, 1994. **12**: p. 991-1045.
89. Land, W.G. and K. Messmer, *The danger theory in view of the injury hypothesis: 20 years later.* Frontiers in Immunology, 2012. **3**.
90. Kono, H. and K.L. Rock, *How dying cells alert the immune system to danger.* Nature Reviews Immunology, 2008. **8**(4): p. 279-289.
91. Rubartelli, A. and M.T. Lotze, *Inside, outside, upside down: damage-associated molecular-pattern molecules (DAMPs) and redox.* Trends in Immunology, 2007. **28**(10): p. 429-436.

92. Gallucci, S., M. Lolkema, and P. Matzinger, *Natural adjuvants: Endogenous activators of dendritic cells.* Nature Medicine, 1999. **5**(11): p. 1249-1255.
93. Scheibner, K.A., et al., *Hyaluronan fragments act as an endogenous danger signal by engaging TLR2.* Journal of Immunology, 2006. **177**(2): p. 1272-1281.
94. Andersson, U., H. Yang, and H. Harris, *High-mobility group box 1 protein (HMGB1) operates as an alarmin outside as well as inside cells.* Seminars in Immunology, 2018. **38**(C): p. 40-48.
95. Rodriguez-Nuevo, A. and A. Zorzano, *The sensing of mitochondrial DAMPs by non-immune cells.* Cell Stress, 2019. **3**(6): p. 195-207.
96. Dubaniewicz, A., *Microbial and human heat shock proteins as 'danger signals' in sarcoidosis.* Human Immunology, 2013. **74**(12): p. 1550-1558.
97. Rock, K.L., H. Kataoka, and J.J. Lai, *Uric acid as a danger signal in gout and its comorbidities.* Nature Reviews Rheumatology, 2013. **9**(1): p. 13-23.
98. Nair, P.N.R., U. Sjogren, and G. Sundqvist, *Cholesterol crystals as an etiological factor in non-resolving chronic inflammation: an experimental study in guinea pigs.* European Journal of Oral Sciences, 1998. **106**(2): p. 644-650.
99. Chen, J.W., et al., *The Immunological Basis in the Pathogenesis of Gout.* Iranian Journal of Immunology, 2017. **14**(2): p. 90-98.
100. Martinon, F., et al., *Gout-associated uric acid crystals activate the NALP3 inflammasome.* Nature, 2006. **440**(7081): p. 237-41.
101. Tublin, J.M., et al., *Getting to the Heart of Alzheimer Disease.* Circulation Research, 2019. **124**(1): p. 142-149.
102. Pollard, K.M., *Silica, Silicosis, and Autoimmunity.* Frontiers in Immunology, 2016. **7**.
103. Tsugo, K., A. Kashimura, and Y. Une, *Asbestosis in a Japanese Macaque (Macaca fuscata).* Toxicologic Pathology, 2015. **43**(7): p. 1035-1039.
104. Fernandes, A.P. and A. Holmgren, *Glutaredoxins: Glutathione-dependent redox enzymes with functions far beyond a simple thioredoxin backup system.* Antioxidants & Redox Signaling, 2004. **6**(1): p. 63-74.
105. Tschopp, J. and K. Schroder, *NLRP3 inflammasome activation: the convergence of multiple signalling pathways on ROS production?* Nature Reviews Immunology, 2010. **10**(3): p. 210-215.
106. Blasius, A.L. and B. Beutler, *Intracellular Toll-like Receptors.* Immunity, 2010. **32**(3): p. 305-315.
107. O'Neill, L.A.J., *The interleukin-1 receptor/Toll-like receptor superfamily: 10 years of progress.* Immunological Reviews, 2008. **226**: p. 10-18.
108. Takeda, K., T. Kaisho, and S. Akira, *Toll-like receptors.* Annual Review of Immunology, 2003. **21**: p. 335-376.
109. Lu, A. and H. Wu, *Structural mechanisms of inflammasome assembly.* Febs Journal, 2015. **282**(3): p. 435-444.
110. Ting, J.P.Y., et al., *The NLR gene family: A standard nomenclature.* Immunity, 2008. **28**(3): p. 285-287.
111. Martinon, F. and J. Tschopp, *Inflammatory caspases and inflammasomes: master switches of inflammation.* Cell Death Differ, 2007. **14**(1): p. 10-22.
112. Martinon, F., K. Burns, and J. Tschopp, *The inflammasome: A molecular platform triggering activation of inflammatory caspases and processing of proIL-beta.* Molecular Cell, 2002. **10**(2): p. 417-426.
113. Barker, B.R., D.J. Taxman, and J.P.Y. Ting, *Cross-regulation between the IL-1 beta/IL-18 processing inflammasome and other inflammatory cytokines.* Current Opinion in Immunology, 2011. **23**(5): p. 591-597.
114. Cullen, S.P., et al., *Diverse Activators of the NLRP3 Inflammasome Promote IL-1beta Secretion by Triggering Necrosis.* Cell Rep, 2015. **11**(10): p. 1535-48.

115. Jo, E.K., et al., *Molecular mechanisms regulating NLRP3 inflammasome activation.* Cell Mol Immunol, 2016. **13**(2): p. 148-59.
116. Jin, C.C. and R.A. Flavell, *Molecular Mechanism of NLRP3 Inflammasome Activation.* Journal of Clinical Immunology, 2010. **30**(5): p. 628-631.
117. Mendonca, R., A.A.A. Silveira, and N. Conran, *Red cell DAMPs and inflammation.* Inflammation Research, 2016. **65**(9): p. 665-678.
118. Figueiredo, R.T., et al., *Characterization of heme as activator of Toll-like receptor 4.* The Journal of biological chemistry, 2007. **282**(28): p. 20221-9.
119. Lin, S., et al., *Heme activates TLR4-mediated inflammatory injury via MyD88/TRIF signaling pathway in intracerebral hemorrhage.* Journal of Neuroinflammation, 2012. **9**.
120. Bevilacqua, M.P., et al., *Interleukin-1 Acts on Cultured Human Vascular Endothelium to Increase the Adhesion of Polymorphonuclear Leukocytes, Monocytes, and Related Leukocyte Cell-Lines.* Journal of Clinical Investigation, 1985. **76**(5): p. 2003-2011.
121. Pohlman, T.H., et al., *An endothelial cell surface factor(s) induced in vitro by lipopolysaccharide, interleukin 1, and tumor necrosis factor-alpha increases neutrophil adherence by a CDw18-dependent mechanism.* J Immunol, 1986. **136**(12): p. 4548-53.
122. Wagener, F.A., et al., *Heme induces the expression of adhesion molecules ICAM-1, VCAM-1, and E selectin in vascular endothelial cells.* Proc Soc Exp Biol Med, 1997. **216**(3): p. 456-63.
123. Belcher, J.D., et al., *Heme triggers TLR4 signaling leading to endothelial cell activation and vaso-occlusion in murine sickle cell disease.* Blood, 2014. **123**(3): p. 377-90.
124. Li, Q., et al., *Heme induces IL-1beta secretion through activating NLRP3 in kidney inflammation.* Cell Biochem Biophys, 2014. **69**(3): p. 495-502.
125. Ng, G., et al., *Receptor-independent, direct membrane binding leads to cell-surface lipid sorting and Syk kinase activation in dendritic cells.* Immunity, 2008. **29**(5): p. 807-18.
126. Sikora, J., et al., *Hemolysis is a primary ATP-release mechanism in human erythrocytes.* Blood, 2014. **124**(13): p. 2150-2157.
127. Dubyak, G.R., *Signal transduction by P2-purinergic receptors for extracellular ATP.* Am J Respir Cell Mol Biol, 1991. **4**(4): p. 295-300.
128. Idzko, M., D. Ferrari, and H.K. Eltzschig, *Nucleotide signalling during inflammation.* Nature, 2014. **509**(7500): p. 310-317.
129. Perregaux, D.G., et al., *ATP acts as an agonist to promote stimulus-induced secretion of IL-1 beta and IL-18 in human blood.* Journal of Immunology, 2000. **165**(8): p. 4615-4623.
130. Chahwala, S.B. and L.C. Cantley, *Extracellular Atp Induces Ion Fluxes and Inhibits Cell-Growth of Murine Erythroleukemia-Cells.* British Journal of Cancer, 1984. **50**(2): p. 249-250.
131. Constantinescu, P., et al., *P2X7 receptor activation induces cell death and microparticle release in murine erythroleukemia cells.* Biochimica Et Biophysica Acta-Biomembranes, 2010. **1798**(9): p. 1797-1804.
132. Wang, B. and R. Sluyter, *P2X7 receptor activation induces reactive oxygen species formation in erythroid cells.* Purinergic Signalling, 2013. **9**(1): p. 101-112.
133. Cayrol, C. and J.P. Girard, *IL-33: an alarmin cytokine with crucial roles in innate immunity, inflammation and allergy.* Current Opinion in Immunology, 2014. **31**: p. 31-37.
134. Bu, X.M., et al., *IL-33 reflects dynamics of disease activity in patients with autoimmune hemolytic anemia by regulating autoantibody production.* Journal of Translational Medicine, 2015. **13**.
135. Wei, J.X., et al., *Red Blood Cells Store and Release Interleukin-33.* Journal of Investigative Medicine, 2015. **63**(6): p. 806-810.
136. Griesenauer, B. and S. Paczesny, *The ST2/IL-33 Axis in Immune Cells during Inflammatory Diseases.* Front Immunol, 2017. **8**: p. 475.
137. Simak, J. and M.P. Gelderman, *Cell membrane microparticles in blood and blood products: potentially pathogenic agents and diagnostic markers.* Transfus Med Rev, 2006. **20**(1): p. 1-26.

138. Tantawy, A.A.G., et al., *Flow cytometric assessment of circulating platelet and erythrocytes microparticles in young thalassemia major patients: relation to pulmonary hypertension and aortic wall stiffness.* European Journal of Haematology, 2013. **90**(6): p. 508-518.
139. Camus, S.M., et al., *Circulating cell membrane microparticles transfer heme to endothelial cells and trigger vasoocclusions in sickle cell disease.* Blood, 2015. **125**(24): p. 3805-3814.
140. Donadee, C., et al., *Nitric Oxide Scavenging by Red Blood Cell Microparticles and Cell-Free Hemoglobin as a Mechanism for the Red Cell Storage Lesion.* Circulation, 2011. **124**(4): p. 465-U294.
141. Zecher, D., A. Cumpelik, and J.A. Schifferli, *Erythrocyte-Derived Microvesicles Amplify Systemic Inflammation by Thrombin-Dependent Activation of Complement.* Arteriosclerosis Thrombosis and Vascular Biology, 2014. **34**(2): p. 313-320.
142. Awojoodu, A.O., et al., *Acid sphingomyelinase is activated in sickle cell erythrocytes and contributes to inflammatory microparticle generation in SCD.* Blood, 2014. **124**(12): p. 1941-1950.
143. Merle, N.S., et al., *Characterization of Renal Injury and Inflammation in an Experimental Model of Intravascular Hemolysis.* Frontiers in Immunology, 2018. **9**.
144. Winterbourn, C.C., *Oxidative Reactions of Hemoglobin.* Methods in Enzymology, 1990. **186**: p. 265-272.
145. Meng, F.T. and A.I. Alayash, *Determination of extinction coefficients of human hemoglobin in various redox states.* Analytical Biochemistry, 2017. **521**: p. 11-19.
146. Rifkind, R.A., *Heinz body anemia: an ultrastructural study. II. Red cell sequestration and destruction.* Blood, 1965. **26**(4): p. 433-48.
147. Rifkind, R.A. and D. Danon, *Heinz Body Anemia--an Ultrastructural Study. I. Heinz Body Formation.* Blood, 1965. **25**: p. 885-96.
148. Clemens, M.R., H. Remmer, and H.D. Waller, *Phenylhydrazine-induced lipid peroxidation of red blood cells in vitro and in vivo: monitoring by the production of volatile hydrocarbons.* Biochem Pharmacol, 1984. **33**(11): p. 1715-8.
149. Rosas, M., et al., *The myeloid 7/4-antigen defines recently generated inflammatory macrophages and is synonymous with Ly-6B (vol 88, pg 169, 2010).* Journal of Leukocyte Biology, 2011. **90**(5): p. 1035-1035.
150. Muller, A., et al., *Hazard classification of chemicals inducing haemolytic anaemia: An EU regulatory perspective.* Regulatory Toxicology and Pharmacology, 2006. **45**(3): p. 229-241.
151. Harel, S. and J. Kanner, *The generation of ferryl or hydroxyl radicals during interaction of haemproteins with hydrogen peroxide.* Free radical research communications, 1988. **5**(1): p. 21-33.
152. Patel, R.P., et al., *Redox cycling of human methaemoglobin by H2O2 yields persistent ferryl iron and protein based radicals.* Free radical research, 1996. **25**(2): p. 117-23.
153. Kosiborod, M., et al., *The relationship between anemia, change in hematocrit over time and change in health status in patients with heart failure after myocardial infarction.* Journal of Cardiac Failure, 2008. **14**(1): p. 27-34.
154. Gouveia, Z., et al., *Characterization of plasma labile heme in hemolytic conditions.* FEBS J, 2017. **284**(19): p. 3278-3301.
155. Welbourn, E.M., et al., *The mechanism of formation, structure and physiological relevance of covalent hemoglobin attachment to the erythrocyte membrane.* Free Radical Biology and Medicine, 2017. **103**: p. 95-106.
156. Camejo, G., et al., *Hemin binding and oxidation of lipoproteins in serum: mechanisms and effect on the interaction of LDL with human macrophages.* Journal of Lipid Research, 1998. **39**(4): p. 755-766.
157. Leal, J.K.F., M.J.W. Adjobo-Hermans, and G. Bosman, *Red Blood Cell Homeostasis: Mechanisms and Effects of Microvesicle Generation in Health and Disease.* Front Physiol, 2018. **9**: p. 703.

158. Chen, G., et al., *Heme-induced neutrophil extracellular traps contribute to the pathogenesis of sickle cell disease.* Blood, 2014. **123**(24): p. 3818-27.
159. Dutra, F.F. and M.T. Bozza, *Heme on innate immunity and inflammation.* Front Pharmacol, 2014. **5**: p. 115.
160. Schroder, K. and J. Tschopp, *The inflammasomes.* Cell, 2010. **140**(6): p. 821-32.
161. Compare, D., et al., *Gut--liver axis: the impact of gut microbiota on non alcoholic fatty liver disease.* Nutr Metab Cardiovasc Dis, 2012. **22**(6): p. 471-6.
162. Szabo, G. and J. Petrasek, *Inflammasome activation and function in liver disease.* Nat Rev Gastroenterol Hepatol, 2015. **12**(7): p. 387-400.
163. Balla, J., et al., *Endothelial-cell heme uptake from heme proteins: induction of sensitization and desensitization to oxidant damage.* Proc Natl Acad Sci U S A, 1993. **90**(20): p. 9285-9.
164. Jeney, V., et al., *Pro-oxidant and cytotoxic effects of circulating heme.* Blood, 2002. **100**(3): p. 879-87.
165. Potor, L., et al., *Atherogenesis may involve the prooxidant and proinflammatory effects of ferryl hemoglobin.* Oxid Med Cell Longev, 2013. **2013**: p. 676425.
166. Chavarria-Smith, J. and R.E. Vance, *The NLRP1 inflammasomes.* Immunological Reviews, 2015. **265**(1): p. 22-34.
167. Duncan, J.A. and S.W. Canna, *The NLRC4 Inflammasome.* Immunological Reviews, 2018. **281**(1): p. 115-123.
168. Latz, E., T.S. Xiao, and A. Stutz, *Activation and regulation of the inflammasomes.* Nat Rev Immunol, 2013. **13**(6): p. 397-411.
169. Lugrin, J. and F. Martinon, *The AIM2 inflammasome: Sensor of pathogens and cellular perturbations.* Immunological Reviews, 2018. **281**(1): p. 99-114.
170. Erdei, J., et al., *Induction of NLRP3 Inflammasome Activation by Heme in Human Endothelial Cells.* Oxid Med Cell Longev, 2018. **2018**: p. 4310816.
171. Soares, M.P., R. Gozzelino, and S. Weis, *Tissue damage control in disease tolerance.* Trends Immunol, 2014. **35**(10): p. 483-94.
172. Reeder, B.J., et al., *Tyrosine as a redox-active center in electron transfer to ferryl heme in globins.* Free radical biology & medicine, 2008. **44**(3): p. 274-83.

PUBLICATION LIST

UNIVERSITY AND NATIONAL LIBRARY
UNIVERSITY OF DEBRECEN
H-4002 Egyetem tér 1, Debrecen
Phone: +3652/410-443, email: publikaciok@lib.unideb.hu

Registry number: DEENK/142/2020.PL
Subject: PhD Publikációs Lista

Candidate: Benard Bogonko Nyakundi
Neptun ID: FE5W81
Doctoral School: Doctoral School of Molecular Cellular and Immune Biology

List of publications related to the dissertation

1. Nyakundi, B. B., Erdei, J. Z., Tóth, A., Balogh, E., Nagy, A., Nagy, B. J., Novák, L., Bognár, L., Paragh, G., Kappelmayer, J., Jeney, V.: Formation and Detection of Highly Oxidized Hemoglobin Forms in Biological Fluids during Hemolytic Conditions.
   Oxidative Medicine and Cellular Longevity. 2020, 1-13, 2020.
   DOI: http://dx.doi.org/10.1155/2020/8929020
   IF: 4.868 (2018)
2. Nyakundi, B. B., Tóth, A., Balogh, E., Nagy, B. J., Erdei, J. Z., Ryffel, B., Paragh, G., Cordero, M. D., Jeney, V.: Oxidized hemoglobin forms contribute to NLRP3 inflammasome-driven IL1[beta] production upon intravascular hemolysis.
   Biochim. Biophys. Acta Mol. Basis. Dis. 1865 (2), 464-475, 2019.
   DOI: http://dx.doi.org/10.1016/j.bbadis.2018.10.030
   IF: 4.328 (2018)

UNIVERSITY AND NATIONAL LIBRARY
UNIVERSITY OF DEBRECEN
H-4002 Egyetem tér 1, Debrecen
Phone: +3652/410-443, email: publikaciok@lib.unideb.hu

List of other publications

3. Erdei, J. Z., Tóth, A., Nagy, A., Nyakundi, B. B., Fejes, Z., Nagy, B. J., Novák, L., Bognár, L., Balogh, E., Paragh, G., Kappelmayer, J., Bácsi, A., Jeney, V.: The Role of Hemoglobin Oxidation Products in Triggering Inflammatory Response Upon Intraventricular Hemorrhage in Premature Infants.
Front. Immunol. 11, 228, 2020.
DOI: http://dx.doi.org/10.3389/fimmu.2020.00228
IF: 4.716 (2018)

4. Erdei, J. Z., Tóth, A., Balogh, E., Nyakundi, B. B., Bányai, E., Ryffel, B., Paragh, G., Cordero, M. D., Jeney, V.: Induction Of NLRP3 Inflammasome Activation By Heme In Human Endothelial Cells.
Oxidative Med. Cell. Longev. 2018, 1-14, 2018.
DOI: https://doi.org/10.1155/2018/4310816
IF: 4.868

Total IF of journals (all publications): 18,78
Total IF of journals (publications related to the dissertation): 9,196

The Candidate's publication data submitted to the iDEa Tudóstér have been validated by DEENK on the basis of the Journal Citation Report (Impact Factor) database.

08 May, 2020

DEBRECENI EGYETEM
Egyetemi és Nemzeti Könyvtár

APPENDIX